Author response to anonymous referee #1

We thank reviewer #1 for his/her thorough and careful review of our manuscript. Below we reply to the reviewer's comments point by point. We list the original comments in black, our replies in blue, major changes or additions to the manuscript in red.

Major comments

1) The introduction should be expanded, particularly the major conclusions and findings in previous work from the same group, and then the unique of this study can be highlighted.

We have expanded the introduction as detailed below.

Page 19408, line 10, *addition to main manuscript*:

We have previously deployed a high resolution aerosol mass spectrometer (HR-ToF-AMS) at the supersite of the Hong Kong University of Science and Technology (HKUST) to determine typical variations in submicron species concentrations, overall composition, size distributions, PMF-resolved organic factors and degree of oxygenation. The supersite measurements provided valuable insights into characteristics of mainly of secondary components of submicron particulate matter, with dominance of sulfate and oxygenated organic aerosol species observed [Lee et al., 2013; Li et al., 2013, 2015]. Subsequent work was conducted at a downtown location in Hong Kong, next to the roadside to assess important primary aerosol sources in the inner-city to identify contributions of long-range transport to roadside pollution, and to establish characteristic concentration trends at different temporal scales. Cooking aerosol was identified as the dominant component in submicron non-refractory organics, followed by traffic-related emissions [Lee et al., 2015]. However, the campaign was conducted in spring and summer of 2013, when PM levels are typically lower than in fall and winter.

The current work focuses on the characterization of roadside aerosol during the fall and winter seasons, when the influence of transported air mass is greatest and PM pollution in Hong Kong is generally

more severe. Episodic haze events were found to be mainly driven by secondary aerosol rather than primary emissions, while day-to-day high PM concentrations were often driven by cooking aerosol. Furthermore, the sources of organic components were investigated in detail, especially SV-OOA. Traffic emissions, local cooking emissions and transported aerosol are all associated with the source of SV-OOA at Mong Kong.

2) Concerning ACSM calibration, did the authors use ammonium sulfate to calibrate RIE(SO4)? Or did the authors have a period of simultaneous measurements between HR-ToF-AMS and ACSM for the intercomparison? The interpretation of ACSM nitrate and sulfate needs to be cautious, particularly sulfate.

We have conducted RIE (SO4) calibrations and obtained an average value of 1.19, rounded up to 1.2, which is exactly the default RIE value. This has been mentioned in the supplementary information of our original submission "The ammonium RIE of 4.57 and sulfate RIE of 1.2 were chosen based on the average from five IE 17 calibrations".

We also did a brief comparison of HR-ToF-AMS and ACSM measurements between August 25 and August 29, with all measured NR-PM1 species correlating well with a Pearson's R values of more than 0.9. The average ratio of SO4, NO3, NH4 and organics of ACSM to that of AMS are 0.90, 0.88, 0.78 and 1.01 respectively as shown in the graphs below. The mass of chloride measured by AMS is much lower than that of ACSM. Howver, as the concentration of chloride during the sampling period was very low in general, we did not discuss chloride trends in this paper.

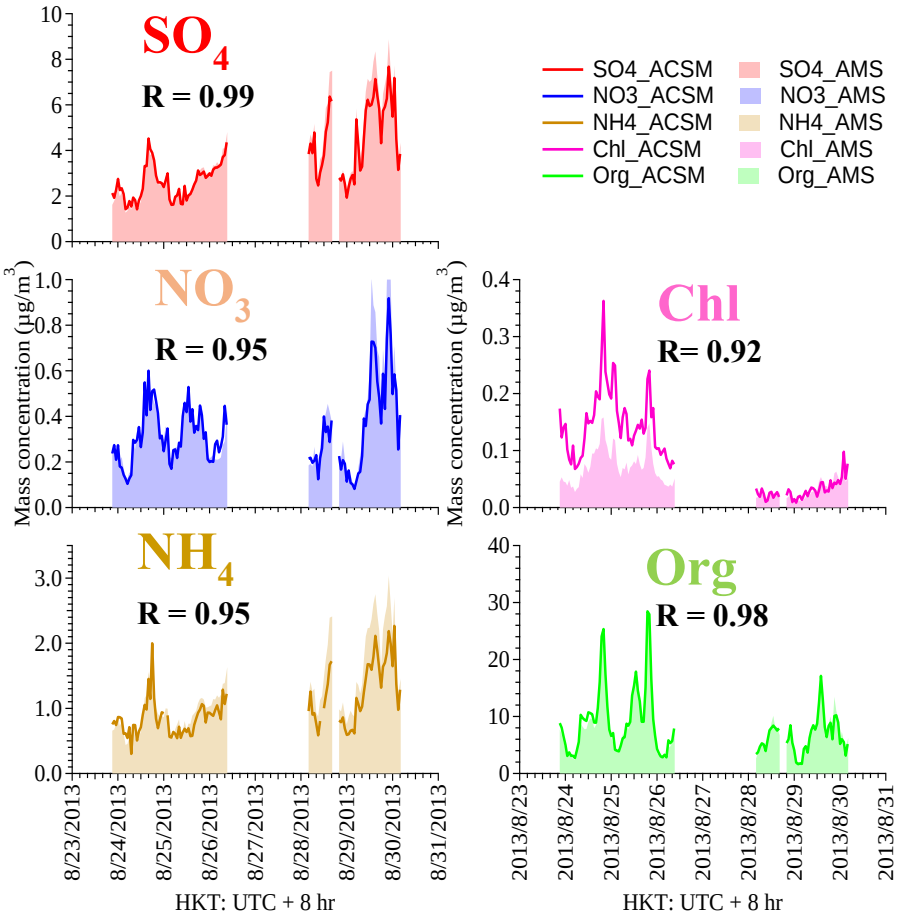

3) Fig. 9 and Fig. 10 were repeated. It's not necessary to use two figures (hourly and daily) to demonstrate the variations and roles of COA. In fact, the time series of Fig. 1b clearly shows that high NR-PM1 peaks were corresponding to high COA. In addition, when plotting Fig. 9, please be careful with the number of points for each bin. Interpreting the data above 60 ug m-3 in Fig. 9 should be careful because Fig. 1b shows a few points above 60 ug m-3.

We agree that the time series of Fig. 1b illustrates the good correlation between NR-PM1 peaks and COA peaks quite well. However, we believe that showing the relationship between the two just from the time series data of Figure 1b does not capture the whole picture. We essentially aim at using Figures 9 and 10 to examine how the PM components are responsible for episodes in different time scales, i.e., hourly basis as shown in Figure 9 and daily basis as shown in Figure

10. In fact, we found that COA showed a significant short-time impact on high hourly PM1 but less impact in daily concentrations in long-time haze events.

The number of individual data for the last two points with the average NR-PM1 concentration exceeding 60 ug/m^3 is 38 and 11, respectively. They cover in total 26 days. We therefore consider them representative.

Minor comments

1. Fig. 1b appears to be stacked plot, please describe it in the caption.

We agree and will modify the manuscript accordingly.

2. Table 4. “four chosen periods” should be “five chosen periods”.

This will be changed in the revised manuscript.

3. Page 19411 Line 22-27: this paragraph can be revised and moved to “experimental” section, e.g., after line 3 in page 19409.

This has been changed in the revised manuscript.

4. Page 19413 Line 11-15: It’s not consistent with Figure 5 that shows diesel-fueled vehicles are the major means during this time range.

It is correct that the number of diesel-fueled vehicles was slightly higher than that of LPG-fueled ones (mainly taxis) between 10 pm and 4am. However, as discussed in the manuscript, leakage of LPG especially during refueling, is another notable source of emissions apart from the usual on-road driving emissions. The intense butane concentrations observed in the nighttime are likely related to leakage, as

refueling of LPG-fueled taxis often takes place in the late night and early morning hours. To clarify this point, we will add the following to the concerned paragraph.

Page 19413, line 14, *addition to main manuscript*:

Furthermore, fuel leakage during refueling of LPG vehicles may contribute more than diesel-fueled vehicular emissions to butane even though the number of diesel fueled vehicles is slightly higher than LPG ones at that time

5. Page 19415 Line 1-10: Interpreting the f44 in the spectra need to be very careful.
ACSM has large uncertainties in determining f44, and often presents significantly higher value than HR-ToF-AMS (see Crenn et al., AMTD, 8, 9239-7302, 2015 and Frohlich et al. AMT, 8, 2555-2576, 2015). Therefore, higher f44 in SV-OOA than "standard SV-OOA" might be simply due to the ACSM uncertainties.

We compared our resolved mass spectra of SV-OOA with standard ones obtained by Q-AMS rather than HR-ToF–AMS, as both Q-AMS and ACSM share the same quadrupole MS technique.

We acknowledge that uncertainties of ACSM and Q-AMS in the f44 determination can play a role and have added this to the concerned paragraph.

Page 19415, line 10, *addition to main manuscript*:

Compared to HR-ToF-AMS measurements, ACSM resolved organic spectra have been observed to show higher f44 in other studies (Crenn et al, 2015, Frohlich et al., 2015) due to inherent instrumental uncertainties in the determination of f44. This might have caused the elevated f44 observed in our SV-OOA spectrum.

Response to anonymous referee #2

We thank reviewer #2 for the thorough and careful review of our manuscript. Below we reply to the reviewer's comments point by point. We list the comments in black, our replies in blue, major changes or additions to the manuscript in red.

Main Comments

1) In page 19410, line 8-9 and in the PMF component spectra it is clear that the observed organic aerosol contains significant levels of m/z 60 and 73. The large body of AMS literature has shown that these ions are typically indicative of influence from biomass burning organic aerosol. These ions have also been used in ACSM studies to show biomass influence (A simple internet search with the keywords "biomass burning ACSM factor", for example, brings up several of the pertinent literature publications). Thus, it is very surprising that the authors do not mention this possibility in the organic aerosol analysis. Why is biomass burning discounted as a source? Some ideas on how the authors can check for the influence of biomass are:

We agree that the presence of m/z 60 and 73 in SV-OOA is unusual. In fact, we tried to separate a biomass burning factor from our PMF analysis but it did not yield satisfactory results. We will give more details in the response to comment #2 further below. We analyzed the source of m/z 60 and 73 but have not included these results in the manuscript. We attribute m/z 60 and 73 in Mong Kok mainly to local cooking activities and long-range transport. The similar diurnal pattern and well matched peaks in the time series data between m/z 60, m/z 73 and COA indicate that cooking emissions contribute part of m/z 60 (Fig 1). Furthermore, LV-OOA tracks very well with the baseline of m/z 60 and m/z 73 as shown in Fig 2, illustrating the partial contribution of long range transport to m/z 60 and m/z 73. Consequently, the sum of LV-OOA and COA shows a better correlation with m/z 60 (Rpr=0.72) and m/z 73 (Rpr=0.78) than each single factor as shown in Table 1. In addition, there are no notable biomass burning sources around the Mong Kok site, which is urban in nature without agricultural or domestic burning practices. Thus a local source of BBOA is very unlikely. Based on above information, we conclude that m/z 60 and 73, marker fragments of BBOA, were mainly imbedded in cooking emissions and transported aerosol rather than a distinct source.

Page 19410, line 4, *addition and modification to main manuscript*:

We note that m/z 60 and 73, important makers of BBOA mass spectra (Aiken et al., 2009; Cubision et al., 2011; Huang et al., 2011), were resolved not only in COA but also in SV-OOA. Their presence in SV-OOA is not the result of artifacts from the PMF analysis, but were attributed to the following reasons, with more details shown in the supplement (sect.3-5). Firstly, when PMF was run using only nighttime data (between 0:00 and 6:00), i.e. when there is little COA (Fig. S6), these two ions still persist with similar fractional intensities in SV-OOA as at other times. Secondly, increasing the number of PMF factors and adjusting the fpeak value did not yield a distinct satisfactory BBOA factor. Thirdly, the time series of m/z 60 and 73 show weak correlation with other burning tracers (EC_residual, CO_residual), with Rpr of about 0.2 and 0.4 respectively, but track well with SV-OOA, with Rpr of 0.92 and 0.93 respectively (Figure 3, Table1).

In terms of the possible sources of m/z 60 and 73, we observe that these two ions showed matching peaks with the COA diurnal profile and good correlations with the sum of the time series of COA and LV-OOA, with Rpr of 0.72 and 0.78 respectively. Furthermore, the ratio of the integrated signal at m/z 60 to the total signal in the organic component mass spectrum is 0.48%, which is just slightly higher than the baseline level (0.3%±0.06%) observed in environments without biomass burning influence and with SOA dominance in ambient OA (Cubision et al.,2011). This indicates that these two ions at Mong Kok were mainly imbedded in cooking emissions and background aerosol due to transport rather than in a distinct source with further details shown in the supplement (sect.6).

Section 4: SV-OOA vs BBOA, *addition to supplemental materials*:

In the 4-factor solution, the mass spectra of resolved SV-OOA contain significant fractions of m/z 60 and m/z 73, which are important makers of BBOA mass spectra (Aiken et al., 2009; Cubision et al., 2011; Huang et al., 2011). The resolved SV-OOA spectrum in our study correlates well with both standard SV-OOA and standard BBOA spectra with Rpr of 0.87 and 0.94, respectively (Figure 4). To assess whether a distinct BBOA factor could be resolved, we increased the number of PMF factors from 4 to 6. With a 5-

factor solution, the existing SV-OOA factor was split into factor 1 and factor 4 as shown in figure 5. However, the mass spectrum of factor 1 is very different from that of BBOA, and the time series of factors 1 and 4 show a high correlation with Rpr of 0.8, indicating a common source rather than two different components. For the 6-factor solution, the existing SV-OOA factor was split into factor 1 and factor 4,and the HOA factor was divided into factor 3 and factor 6 (figure 6). The mass spectra of factor 1 and factor 4 are very different from that of standard BBOA with a Ruc of 0.56 and 0.68, respectively. Thus, we are not able to separate a distinct BBOA factor from the existing SV-OOA based on the unit mass resolution data, which is consistent with previous studies conducted in Hong Kong (Li et al., 2011, 2015; Lee et al., 2011, 2015).

Section 5: SV-OOA vs COA, *addition to supplemental materials*:

Apart from SV-OOA, m/z 60 and m/z 73 are also present in the mass spectrum of COA, and they share a similar diurnal pattern with COA (Figure1). To examine the possibility that PMF erroneously assigned these two ions to COA instead of SV-OOA, PMF was run using only nighttime data (between 0:00 and 6:00), when there is only residual COA present (Figure S6). We found that these two ions still persist, with similar fractional intensities in SV-OOA as at other times and have thus been correctly assigned.

On the other hand, the diurnal pattern of SV-OOA also shows matching peaks with COA. To further examine the relationship of the COA factor and SV-OOA factor, PMF was run with 4, 5 and 6 factor solutions respectively. The correlations between COA and SV-OOA like factors decrease (Table 2) as the number of PMF factor increases. However, the mass spectral correlations (Ruc) between resolved COA and standard COA decrease from 0.84 to 0.77, and the correlation of the sum of SV-OOA like factors and standard SV-OOA reduces from 0.87 to 0.79, indicating a reduction of the quality of PMF solution. In addition, the average COA loading decreases from 3.6 to 2.7 $\mu g/m^3$ rather than increase, which suggests that increasing the number of PMF factors does not separate possible COA related components from the SV-OOA like factors.

The effects of varying fpeak on the correlations between SV-OOA and the COA time series from this 4-factor solution were also analyzed. As shown in Tables 3 and4, when the fpeak value changes from 0 to -

0.2 and -0.4, the time series correlation of SV-OOA and COA just decreases slightly, but the mass spectra correlations between resolved COA, SV-OOA and their standards decrease appreciably. When the fpeak value increases from 0 to 0.4, the similarity of COA and SV-OOA times series increase dramatically, and except for LV-OOA the mass spectra correlations between resolved OA factor and their standard profiles all decrease. We acknowledge the limitation and uncertainty of PMF analysis on resolving factors, but considering the resulting mass spectra, the time series data of the loadings and the correlations with standard mass spectra, we consider that the four-factor solution with an fpeak value of 0 is optimal in our case.

Section 6: the source of m/z 60 and 73, *addition to supplemental materials*:

The fractions of signal at m/z 60 and m/z 73 to the total signal of SV-OOA like factors are persistent and remain above 1% as the number of PMF factor increases from 4 to 6 as shown in table 2. In terms of the source of these two ions, the similar diurnal pattern and well matched peaks in the time series data between m/z 60, m/z 73 and COA indicate that cooking emissions contribute part of m/z 60 and m/z 73 (Fig 1). Furthermore, LV-OOA tracks very well with the baseline of m/z 60 and m/z 73 as shown in Figure 2, illustrating the partial of contribution of long-range transport to m/z 60 and m/z 73. The sum of LV-OOA and COA show a better correlation with m/z 60 (Rpr=0.72) and m/z 73 (Rpr=0.78) than each single factor as shown in Table 1, supporting above hypothesis that transport aerosol and local cooking emissions are both sources of m/z 60 and 73 at Mong Kok. In addition, the comparison between m/z 60, 73 and plumes of EC and CO do not correlate well with NOx represented by EC_resiudal and CO_residual (Fig. 3). m/z 60 showed weak correlation with the residual of EC (Rpr=0.37) and CO (Rpr=0.21). A similar weak relation is apparent for m/z 73. Therefore, biomass burning influence around the Mong Kok site is highly unlikely. Also, the ratio of the signal at m/z 60 to the total signal in the OA mass spectrum (0.48%) in this study is just slightly higher than the baseline level (0.3%±0.06%) observed in environments without biomass burning influence and SOA dominance in ambient OA (Cubision et al.,2011). Based on the above analysis, we conclude that m/z 60 and 73, usually marker fragments of BBOA, were mainly imbedded in cooking emissions and transport aerosol rather than a distinct source.

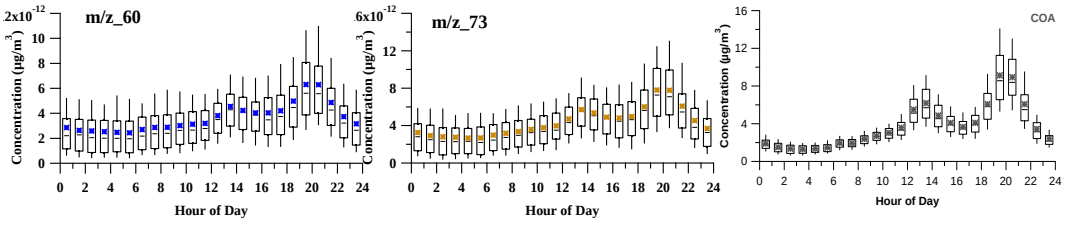

Fig 1. Diurnal pattern of m/z 60, m/z 73 and COA

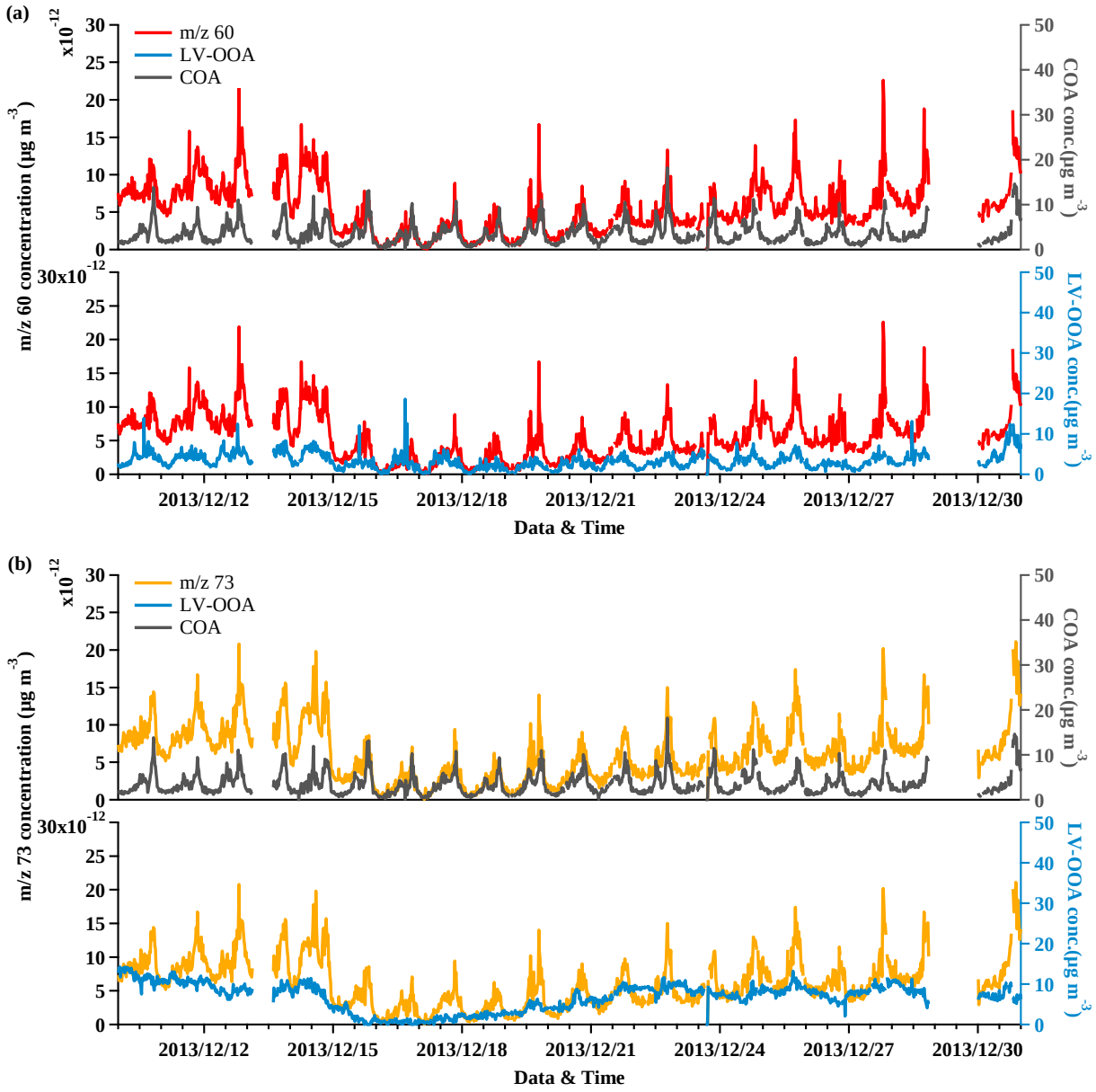

Fig 2. Temporal variation of m/z 60, m/z 73, LV-OOA and COA, excerpt from December, 2013.

Table 1. Correlations of the time series data between m/z 60, 73 and SV-OOA, LV-OOA, COA, sum of LV-OOA and COA, NO3, NH4 and SO4.

Pearson R	SV-OOA	LV-OOA	COA	LV-OOA+COA	NO3	NH4	SO4
m/z60	0.92	0.55	0.49	0.72	0.66	0.59	0.42
m/z73	0.93	0.54	0.58	0.78	0.64	0.57	0.41

The time trends of m/z 60 and m/z 73 can be analyzed and compared to each other as well as external burning tracers such as EC and CO. Plumes of EC and CO that do not correlate with NOx can be used as possibly indication of biomass burning influence

We added the comparison between m/z 60, 73 and plumes of EC and CO that do not correlate with NOx represented by EC_resiudal and CO_residual (Fig. 3). EC_residual and CO_residual are defined as the residual of the equation: EC(or CO) =a* NOx. m/z 60 showed weak correlation with the residual of EC (Rpr=0.37) and CO (Rpr=0.21). The same applies to m/z 73. Therefore, influence of biomass burning at MK is quite unlikely.

Please refer to "**Page 19410, line 4, *addition and modification***" on the response to main comment 1).

"The time series of m/z 60 and 73 show weak correlation with burning tracers (EC_residual, CO_residual), with Rpr of about 0.2 and 0.4 respectively."

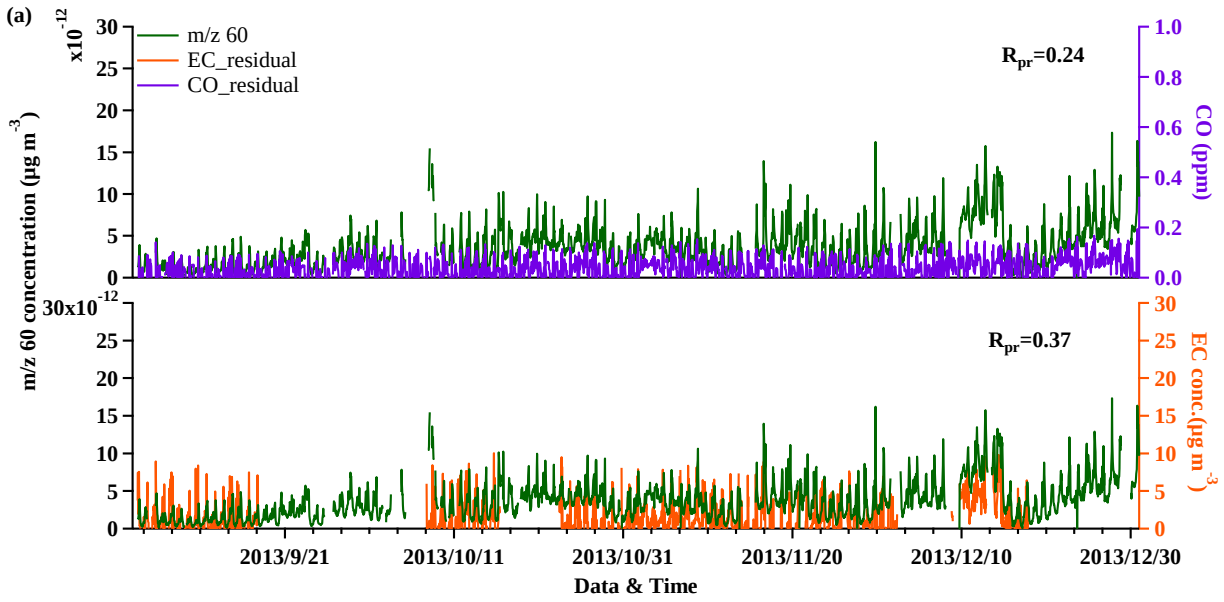

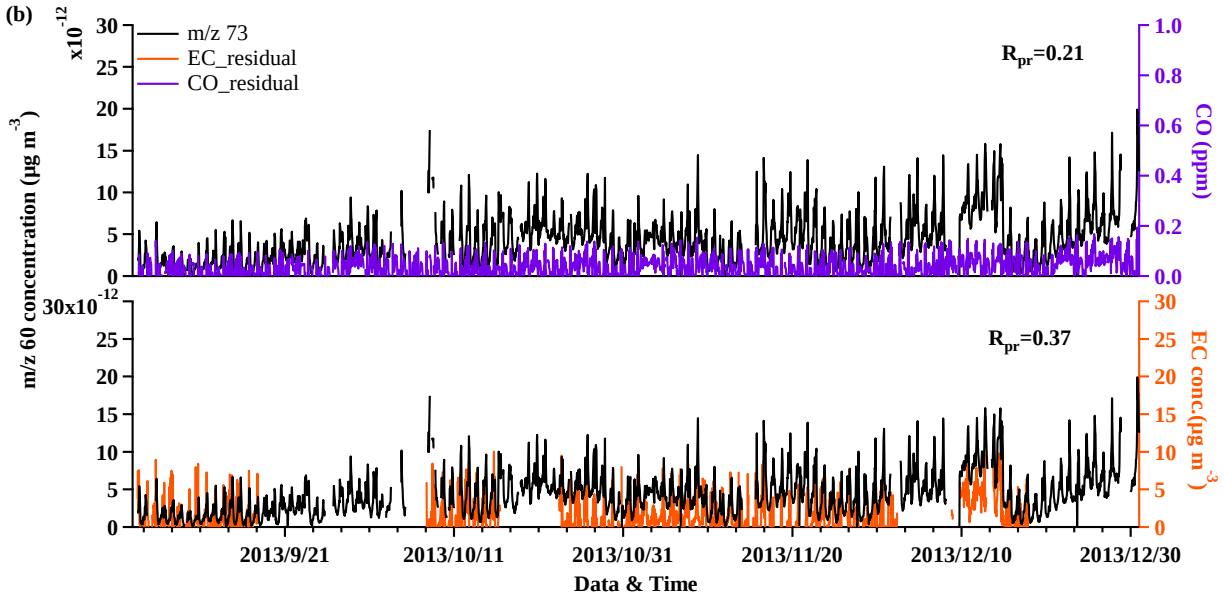

Fig. 3 Time series of m/z 60, m/z 73, EC_residual and CO_residual. Note that EC_residual and CO_residual are defined as the residual of the equation: EC(or CO) =a* NOx.

A manuscript by Cubison et al. has reported f60 values in various air masses with and without biomass influence. The observations from Hong Kong can be compared to those values.

We agree and will expand on the OOA part as detailed below.

Please refer to "**Page 19410, line 4, *addition and modification*"** on the response to main comment 1).

Furthermore, the ratio of the integrated signal at m/z 60 to the total signal in the organic component mass spectrum is 0.48%, which is just slightly higher than the baseline level (0.3%±0.06%) observed in environments without biomass burning influence and SOA dominance in ambient OA (Cubision et al.,2011)

Comparisons of the observed SV-OOA spectrum to "standard" BBOA spectra in spectral databases

We compared the SV-OOA spectrum with the standard ones as shown in the graph below. The resolved SV-OOA spectrum in our study correlates well with both standard SV-OOA and standard BBOA spectra with Rpr of 0.87 and 0.94, respectively. As discussed previously, the BBOA signature ions are mainly attributed to long-range transport and cooking activities rather than local biomass burning. Transport of biomass burning derived pollutants from the PRD region is possible, but would appear as processed OA, i.e. either in form of SV-OOA or LV-OOA. In addition, increasing the number of PMF factors from 3 to 6 (see details below) did not yield a separate BBOA factor. This is consistent with previous studies in Hong Kong (Li et al., 2013, 2015; Lee et al., 2013, 2015) which also could not resolve BBOA.

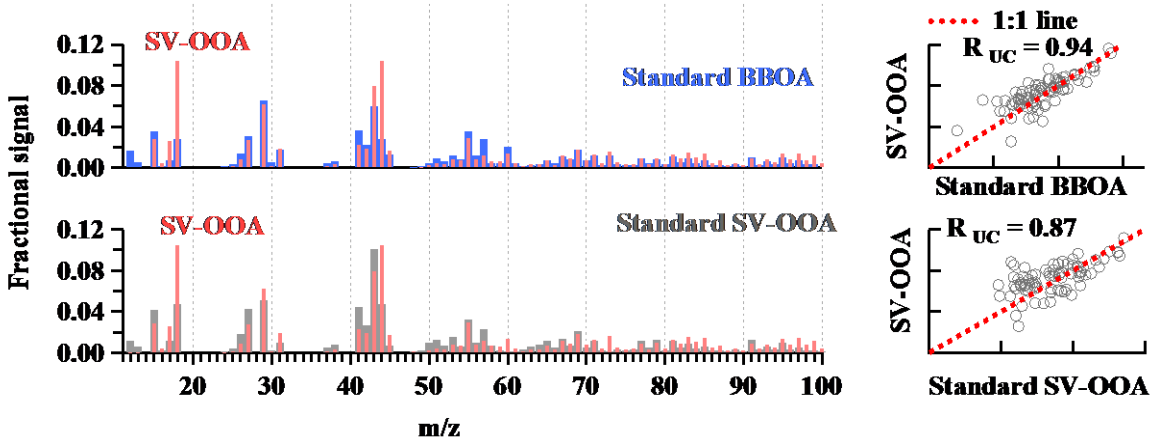

Fig 4. Mass spectra of resolved SV-OOA (pink) in our study and standard mass spectra of BBOA available on the AMS MS database (Ulbrich, I. M., Lechner, M., and Jimenez, J. L., AMS Spectral Database)

Since the SV-OOA component concentration is largely influenced by regional continental transport, and appears to be particularly important in high concentration pollution events, it may be possible to see whether there is any correlation between SV-OOA and other data regarding fires in the region.

We do not have data regarding fires in and beyond the PRD region.

The residuals in the PMF analysis of m/z 60 and m/z 73 can be investigated to see if they perhaps get a lot smaller at a larger number of factors and if perhaps a clean biomass burning factor splits from the existing SV-OOA component at larger factor numbers.

With a 5-factor solution, the existing SV-OOA factor was split into factor 1 and factor 4 as shown in figure 5. However, the mass spectrum of factor 1 is very different from that of BBOA, and the time series of factors 1 and 4 show high correlation with Rpr of 0.8, indicating a common source rather than two different components. For the 6-factor solution, the existing SV-OOA factor was split into factor 1 and factor 4,and HOA was divided into factor 3 and factor 6 (Figure 6)., The mass spectra of factor 1 and factor 4 are very different from that of standard BBOA with a Ruc of 0.56 and 0.68, respectively. Thus, we are not able to separate a distinct BBOA factor from the existing SV-OOA. In addition, the fractions of signal at m/z 60 and m/z 73 to the total signal of SV-OOA like factors do not reduce much as the number of PMF factors increases from 4 to 6 as shown in Table 2.

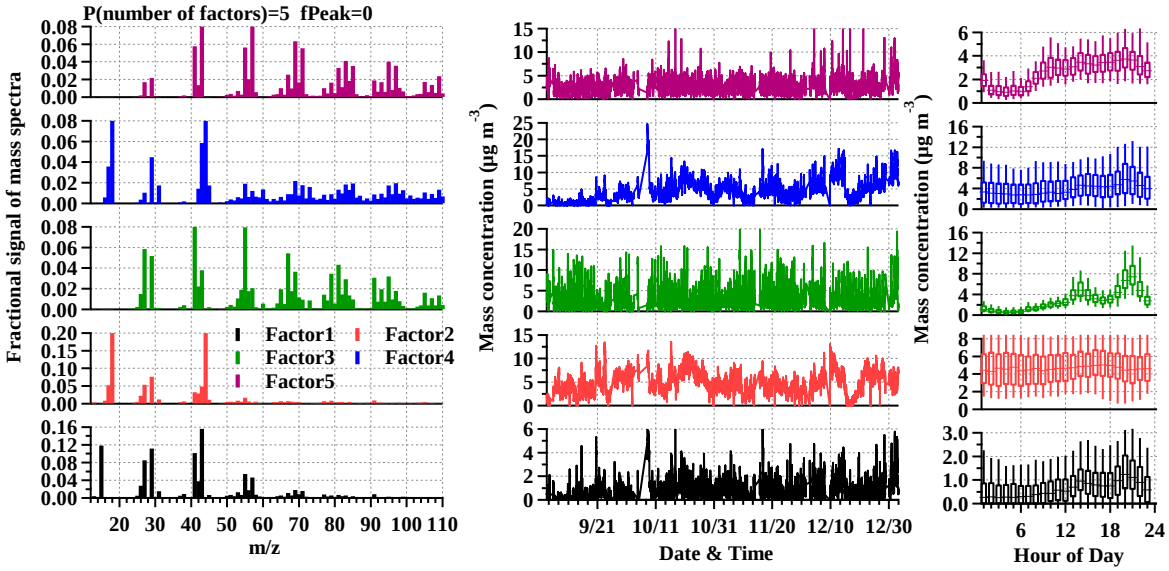

335

336 Figure 5. Mass spectra, time series and diurnal pattern for 5 factors with fPeak=0.

337

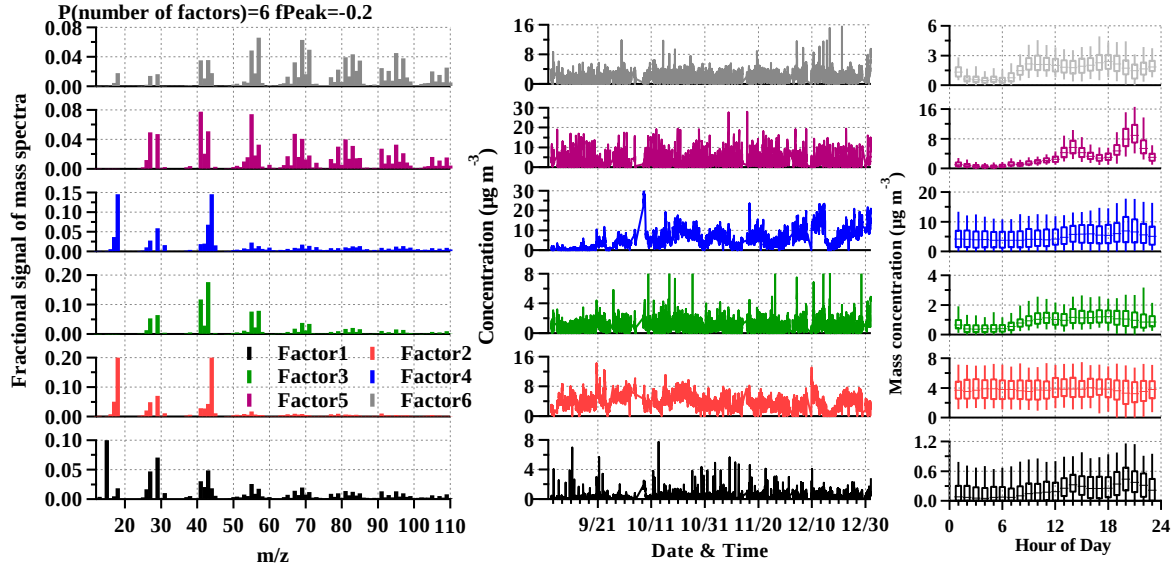

338

339 Figure 6. Mass spectra, time series and diurnal pattern for 6 factor solution with fPeak=-0.2.

340

341

342

343

Table 2. Correlation of resolved OA factor mass spectra and their standard profiles, time series correlation between COA and SV-OOA like factors, fractional signal at m/z 60, 73 to total SV-OOA signal, and the average mass concentration of OA factors for the 4-factor, 5-factor and 6-factor solutions.

	Organic factors	4 factor	5 factor	6 factor
Ruc for mass spectra	COA with standard	0.84	0.76	0.77
	SV-OOA with standard	0.87	0.85	0.79
	HOA with standard	0.93	0.93	0.98
	LV-OOA with standard	0.97	0.97	0.97
Rpr for Time series	COA with SV-OOA like factor 1	0.45	0.36	0.26
	COA with SV-OOA like factor 2		0.39	0.22
	COA with SV-OOA like factor 1+ factor 2		0.37	0.28
Fraction in SV-OOA	m/z 60	1.4%	1.3%	1%
	m/z 73	1.6%	1.5%	1.1%
Concentration ($\mu g/m^3$)	Average COA	3.6	2.6	2.7
	Average SV-OOA	3.1	4.4	5.0
	Average HOA	2.7	2.5	2.3
	Average LV-OOA	5.7	5.2	5.0

2) It is clear from the observed SV-OOA time trends (particularly peaks at 12 pm and 6 pm) that the SV-OOA factor contains some influence of the COA factor. Unless the SV-OOA species are secondary species formed from the cooking process (or other co-located SOA source), there is no other simple reason why SV-OOA should contain this diurnal trend. The authors do not clearly address how they tried to deal with this mixing. This is important considering that the SV-OOA is a significant fraction of the OA. Some questions pertinent to this are:

Did the authors try to go to a much larger number of factors and investigate what happened to the COA loadings and correlation with the SV-OOA-like factor?

Table 2 above summarizes the results of possible 4, 5 and 6 factor solutions from the PMF analysis. When the number of PMF factors increases from 4 to 6, the correlations between COA and SV-OOA like factors show a decrease (Table 2). However, the mass spectral correlations (Ruc) between resolved COA and standard COA decrease from 0.84 to 0.77, and the correlation of the sum of SV-OOA like factors and standard SV-OOA reduces from 0.87 to 0.79. In addition, the average COA loading decreases from 3.6 to 2.7 $\mu g/m^3$ rather than showing an expected increase, which suggests that increasing the number of PMF factors does not separate possible COA related components from the SV-OOA like factors.

We acknowledge the limitation and uncertainty of PMF analysis on resolving factor completely, but considering the resulting mass spectra, the time series data of the loadings and the correlations with standard mass spectra, we consider the four-factor solution as optimal in our case.

Did the authors investigate the effect of fpeak on the time series correlation between SV-OOA and COA. What do the results look like at the fpeak setting where this correlation is minimized?

According to the above analysis, we have identified the 4-factor solution is the most appropriate for our study. The effects of fpeak on the correlations between SV-OOA and COA time series are thus presented for the 4 factor solution. As shown in Tables 3 and 4, when the fpeak value changes from 0 to -0.2 and -0.4 subsequently, the time series correlation of SV-OOA and COA decreases slightly, but the mass spectral correlations between resolved COA, SV-OOA and their standards decrease appreciably. When the fpeak value increases from 0 to 0.4, the similarity of COA and SV-OOA times series increase dramatically, and except for LV-OOA, the mass spectra correlations between the resolved OA factors and their standard profiles all decrease. Thus, an fpeak value of 0 for the 4-factor case considered as the most appropriate solution for the PMF analysis.

Table 3. Time series correlation between resolved SV-OOA and COA for the 4-factor solution for different fpeak values.

Rpr	-0.4	-0.2	0	0.2	0.4

SV-OOA and COA	0.40	0.43	0.45	0.64	0.63

Table 4. Correlation between our resolved PMF factors from the 4-factor solution with standard mass spectra for different fpeak values.

Ruc\fpeak	-0.4	-0.2	0	0.2	0.4
HOA vs STD	0.94	0.94	0.92	0.90	0.88
COA vs STD	0.77	0.77	0.84	0.76	0.75
LV-OOA vs STD	0.98	0.98	0.97	0.97	0.97
SV-OOA vs STD	0.83	0.85	0.87	0.78	0.84

Even if they are unable to use it for this manuscript, the authors should at least mention that ME-2 based analyses like possible with the SOFI tool could be a means of dealing with this.

We have expanded on the Experimental section as detailed below.

Page 19409, line 19, *addition to main manuscript*:

"ME-2 analysis with the SOFI tool as applied in several studies may yield additional insights but has not been applied in this study due to its ongoing development (Canonaco et al., 2013; Minguillón et al., 2015)."

Relevant methods similar to those used by Aiken et al. to evaluate biomass burning in Mexico city (http://www.atmos-chem-phys.net/10/5315/2010/acp-10-5315-2010.pdf) could be attempted.

Aiken et al. used satellite data derived fire counts and FLEXPART modeling, both of which are not available for this study.

3) One weakness of this manuscript is that it reads like a report of AMS/ACSM measurements at yet another field site. It would be useful for the authors to provide as much inter-comparison with other previous measurements as possible to provide a larger con-text within which we can understand these measurements. For example:

The authors mention that transport from PRD can be a source of some of the observed aerosol at the Hong Kong site. How do the loading and composition of the aerosol particles observed at the current site differ from those previously observed in the PRD region? Is it possible, for example, that BBOA from the PRD is a source of the observed m/z 60 and m/z 73 in the ACSM spectra at this site?

These measurements were conducted in the winter and fall. How do the results (absolute concentrations and relative compositions) differ with previous studies at the same site or similar site that were conducted at the same or other seasons?

We will expand on the introduction as detailed below.

Page 19408, line 10, *addition to main manuscript*:

Recently, a high resolution aerosol mass spectrometer (HR-ToF-AMS) was applied at an urban site in the Shenzhen metropolitan area and a rural site in PRD region during October and November (He et al., 2011; Huang et al., 2011). They found that organic concentration dominates followed by sulfate which is similar to this study, but the fraction of sulfate at the rural site is larger than that of the urban site. Four OA components were identified in urban site including HOA, BBOA, LV-OOA and SV-OOA, but only three OA factors without HOA were resolved in rural site. They both reported an important contribution from

BBOA with about 24% of total OA.

We have previously deployed HR-ToF-AMS at the supersite of the Hong Kong University of Science and Technology (HKUST) to determine typical variations in submicron species concentrations, overall composition, size distributions, PMF-resolved organic factors and degree of oxygenation. The supersite measurements provided valuable insights into characteristics of mainly of secondary components of submicron particulate matter, with dominance of sulfate and oxygenated organic aerosol species observed [Lee et al., 2013;Li et al., 2013, 2015]. Subsequent work was conducted at a downtown location (Mong Kok) in Hong Kong, next to the roadside, in spring 2013 to assess important primary aerosol sources in the inner-city to identify contributions of long-range transport to roadside pollution, and to establish characteristic concentration trends at different temporal scales. Cooking aerosol was identified as the dominant component in submicron non-refractory organics, followed by traffic-related emissions [Lee et al., 2015].

This work focuses on the characterization of roadside aerosol during the fall and winter seasons, when the influence of transported air mass is greatest and PM pollution in Hong Kong generally more severe. Episodic haze events were found to be mainly driven by secondary aerosol rather than primary emissions, while hourly high PM concentrations were often driven by cooking aerosol. Statistical methods were employed to show that the correlation of COA and HOA to SV-OOA varied under different conditions and period of a day. While HOA showed a stronger relationship to SV-OOA overall, COA can be an important contributor to SV-OOA during meal times.

Other comments

4) Section 3.2: When the various OA components are described, it would be useful to have the brief description of their mass spectra (which is currently in the supplementary) included in the main manuscript to reinforce the key mass spectral features used in the factor assignments. Similarly, the discussion of the COA that is currently in the supplementary could be moved to the main.

We agree and will modify the manuscript accordingly.

Page 19412, line 12, *addition to main manuscript*:

The mass spectrum of HOA is dominated by the $C_nH_{2n-1}^+$ ion series (m/z 27, 41, 55, 69, 83, 97), typical of cycloalkanes or unsaturated hydrocarbon, which account for 27% of total peak intensity in the HOA spectrum. The other prominent group is the $C_nH_{2n+1}^+$ ion series (m/z 29, 43, 57, 71, 85, 99), typical of alkanes and accounting for 26% of the total peak. This mass spectrum is very similar to the standard HOA spectrum with R_{uc} of 0.92, and its fractions of $C_nH_{2n-1}^+$ and $C_nH_{2n+1}^+$ (27%, 26%) are consistent with standard ones (=28%, 27%) (Ng et al., 2011). This HOA spectrum is also consistent with that resolved by HR-ToF-AMS at the HKUST Supersite on the dominance of saturated CxHy-type ions, most notably at *m/z* 43 and 57 (Lee et al., 2013).

Page 19413, line 19, *addition to main manuscript*:

The most prominent ions of the resolved COA profile at MK were *m/z* 41 (mainly C_2HO^+, $C_3H_5^+$) and *m/z* 55 (mainly $C_3H_3O^+$, $C_4H_7^+$). Ratios of *m/z* 41/43 =1.8 and *m/z* 55/57=2.2, which are distinctly larger than that of HOA at 0.73 and 0.76 respectively (Figure 4); such ratios have been widely reported for COA in AMS and ACSM studies.For example, Lanz et al. (2010) reported ratios of *m/z* 41/43 and *m/z* 55/57 of 0.5 and 0.4 in HOA, and 1.2 and 1.2 in COA, respectively, while Sun et.al (2013) reported 0.5 for these two ratios in HOA and 2.3 for those in COA, respectively.

Page 19414, line 18, *addition to main manuscript*:

LV-OOA is characterized by the prominent m/z 44 ion (mainly CO_2^+) and minor C_nH_{2n-1} and C_nH_{2n+1} ion series generated by saturated alkanes, alkenes and cycloalkanes.

Page 19414, line 24-25, *modification of main manuscript*:

SV-OOA, which is less oxidized than LV-OOA, is marked by the dominant ions of *m/z* 43 and *m/z* 44 mainly contributed by $C_2H_3O^+$ and CO_2^+, The mass spectrum of SV-OOA closely resembles that of

'standard' SV-OOA with a R_{uc} of 0.87 (Fig. 3). Its time series also follows that of nitrate (R_{pr}=0.63, Figure 1), another secondary and semi-volatile species.

5) Page 19415, line 22-19416, line 5: this section is a little long winded. It would be better to cut out a lot of the discussion of the correlation coefficients, which are not really that useful, and instead point out the differences in actual mass concentrations for the different periods that are in the table. While it is useful to have done the HiOx and LOx comparisons, I think it can be summarized in a couple sentences and it is not clear to me that this extended discussion provides any more useful information about the SV-OOA than is possible from the diurnal cycle. So, I would get rid of this aspect of the discussion. It would be better to focus on the types of diagnostics suggested in comment #2 above in the main comment section.

We will make the manuscript more concise on the Table 2 and 3 description as detailed below. However, we consider the discussion of correlation coefficients useful to show their relative importance to SV-OOA under different conditions and help to identify possible reasons for the observed concentration changes.

Page 19416, line 5 to Page 19417, line 5, *modification of main manuscript*:

The average concentrations of HOA and SV-OOA under HTemp are obviously lower than under LTemp for each period but the concentration of COA and LV-OOA varies little across different temperatures (Table2). Combining the stronger correlations between HOA and SV-OOA than between COA and SV-OOA, a stronger and closer temperature dependence of HOA and SV-OOA was revealed. In addition, the regression coefficients of HOA and COA during each period under HTemp (Table 2) are much smaller than under LTemp, reflecting a weakening of their relationship with SV-OOA as temperature increases.

Consistent with the discussion of Fig 7, the concentrations of HOA, SV-OOA and LV-OOA except for COA under HiOx are greatly higher than those under LOx for each period. Besides, HOA shows an increase correlation with SV-OOA under HiOx due to the more intensive oxidation of HOA precursor to SV-OOA. However, LV-OOA shows a reverse trend with smaller coefficients with SV-OOA. It is

probable that HiOx conditions favor the conversion of SV-OOA to LV-OOA leading to smaller coefficient of LV-OOA on SV-OOA, although overall most LV-OOA is considered to be from transport.

At last, we also can conclude that HOA overall has a stronger relationship to SV-OOA than COA has, supported by much higher coefficients of HOA than that of COA over all time periods, and temperature and Ox levels. Cooking emissions are not as important to SV-OOA in the BT periods but they can be important during MT periods, indicated by the lowest concentration and correlation with SV-OOA during BT but highest concentration during MT periods."

6) Page 19418, page 3- Isn't the diurnal variation in aerosol components like Chloride also driven by the boundary layer? Are their measurements of CO that show how much the dilution is during the day? If so, it would be useful to show the CO diurnal trends as well for reference.

As our sampling site is situated in a typical roadside area with heavy influence of traffic emission, the concentration of CO was influenced greatly by traffic emissions, as shown below. In addition, complex and high building structures around the measurement site (street canyon) complicate the effects of circulation and PBL variation and thus we are not able to directly assess the influence of dilution due to changes in PBL height.

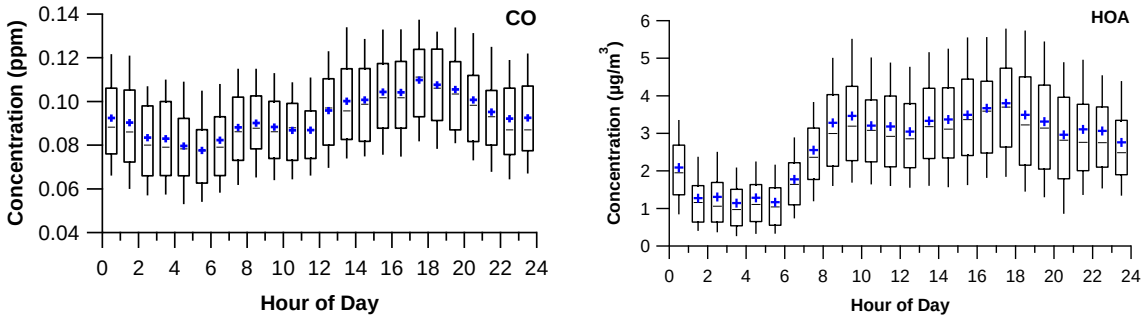

Figure 7. The diurnal pattern of CO and HOA during the whole study.

7) Page 19420- what is the wind direction classification for C2? Is the main difference between C1 and C2 the fact that it rained? If so this should be stated. Also, it would be nice if in the discussion of Table 4,

the periods that should be directly compared with each other due to similarity in source regions or other conditions are explicitly stated. Otherwise, the reader has to try and summarize for themselves the results from the analysis of table 5. It would also help if in Table 4, the source region classification (i.e. continental, coastal etc.) of each period was provided.

The wind direction of C2 is mainly northerly, belonging to continental wind. The main differences in meteorological conditions between C2 and C1 are the occurrence of precipitation, much lower temperature and source region shift from coastal to continental region. According to your comment, Table 4 will be expanded as detailed below and the manuscript will be reorganized.

Page 19420, line19, *modification of main manuscript*:

Although the total NR-PM1 of C1 (12.2 μgm^{-3}) and C2 (11.8 μgm^{-3}) are both only 25–30% of that during haze periods, they were driven by different mechanisms. The main differences in meteorological conditions between C1 and C2 are the dominance of continental wind rather than coastal wind, much lower temperature and the existence of precipitation in C2. The low concentration of C1 is mainly attributed to easterly wind bringing less air pollutants and diluting local air pollutants. To a lesser extent, it is influenced by both particle evaporation, especially for SV-OOA, and dilution of local emissions during high temperatures, which might be the reason why HOA, COA and SV-OOA in C1 are lower than in C2 despite the lack of rain. The low mass loading of C2 was mainly caused by the wet deposition of precipitation. It dramatically reduces the concentration of secondary species such as SO4, NH4, NO3, SV-OOA and LV-OOA, but not primary HOA and COA. Compared to the adjacent period H3, the total organic mass reduces by 68% to an average of 8.1 μgm^{-3} (Table 4). Precipitation effectively removes secondary particles but is less efficient for primary particles that are continuously generated locally.

With similar continental source region as C2, the most severe pollution event H3 occurred during 10–13 December with an average NR-PM1 of 47.7 μgm^{-3}. The persistent northerly wind continually brought air masses from the PRD region into Hong Kong and lead to a marked mass increase of secondary species of SO4, NH4, NO3, LV-OOA and SVOOA. Furthermore, H3 is characterized by the highest mass

concentration and relative contribution of nitrate and SV-OOA compared with other haze periods. This is likely due to the average temperature of H3 being 5–6ºC lower than that of other haze events. In addition, although all three haze events have very similar SO4 mass loading, there is a ~ 50% increase in NH4 concentration during the H3 episode, consistent with the increase of nitrate in that period.

The other two haze events are adjacent with influence from both continental and oceanic region in H1 and continental source region in H2. The mixed pattern of source regions during H1 identified as land–sea breeze (Fig. S8) can redistribute PM pollution over the whole PRD region and accumulate air pollutants effectively (Lo et al., 2006; Chan and Yao, 2008; Lee et al., 2013). The pronounced high concentration of LV-OOA and SV-OOA, jointly contributing 70% of total organics, reflects the oxidation of primary emissions in the PRD under such cycles, which is also observed at the suburban HKUST site (Lee et al., 2013). The periodic nitrate peaks in H1 with low concentration in daytime and high concentration in nighttime coincide with temperature changes. During H2 period, the prevailing wind is northwesterly and there is a sharp decrease in relative humidity. It is interesting to note that the dip in RH during H2 coincides with the dip in sulfate, ammonium, nitrate and LV-OOA; this might be caused by decreased aqueous-phase processing, and by decreased gas-particle partitioning associated with water uptake under low RH for secondary aerosol particles (Sun et al., 2013a, b).

Table 4. Measured and calculated parameters in four chosen periods (C1, H1, H2, H3 and C2)

	Clean period 1 (C1)[a]		Haze period 1 (H1)		Haze period 2 (H2)		Haze period 3 (H3)		Clean period 2 (C2)	
RH (%)	70.8		65.0		36.4		64.8		84.6	
T **(** ^{o}C **)**	27.6		25.0		23.8		18.7		13.2	
O_x (ppb)	69.6		82.0		99.5		70.4		40.9	
***f*44**	0.114		0.118		0.120		0.108		0.057	
Precip(mm)	0		0		0		0		8.9	
Wind	coastal		continental/oceanic		continental		continental		continental	
(μg/m^3, %)	**Conc.**	**Perc.**	**Conc.**	**Perc.**	**Conc.**	**Perc.**	**Conc.**	**Perc.**	**Conc.**	**Perc.**
NR-PM_1	12.2		44.1		39.0		47.7		11.6	
Org	6.7	54.4	25.2	57.2	21.1	54.2	25.1	52.6	8.1	69.6
SO_4	3.8	31.2	11.8	26.8	12.1	30.9	11.4	23.8	1.5	12.8
NH_4	1.2	9.9	4.4	10.1	4.4	11.3	6.5	13.6	1.1	9.4
NO_3	0.4	3.5	2.4	5.6	1.3	3.4	4.4	9.2	0.8	7.3
Chl	0.1	1.0	0.2	0.4	0.1	0.2	0.4	0.8	0.1	0.9
HOA	1.2	18.5	3.8	15.1	3.0	14.4	4.2	16.9	2.1	26.2
COA	2.3	34.8	3.7	14.5	3.3	15.5	3.3	13.1	2.6	31.7
LV-OOA	3.0	44.8	11.5	45.4	10.2	48.4	9.9	39.6	1.8	22.0
SV-OOA	0.1	2.0	6.3	25.0	4.5	21.6	7.6	30.4	1.6	20.1

8) Figure 3: The COA and SV-OOA MS correlations with the reference spectra look quite scattered. This is likely indicative of the fact that the SV-OOA has COA mixed into it. It would be useful in supplementary to show the correlation spectra for SV-OOA and COA with markers corresponding to m/z so that the masses that have discrepancies are more easily identified. Another option would be to draw the reference spectra behind each of the component mass spectra in gray so that the comparison can be readily made by the reader.

We have modified Figure 3 in the manuscript by adding reference spectra behind each of the component mass spectra in gray as detailed below.

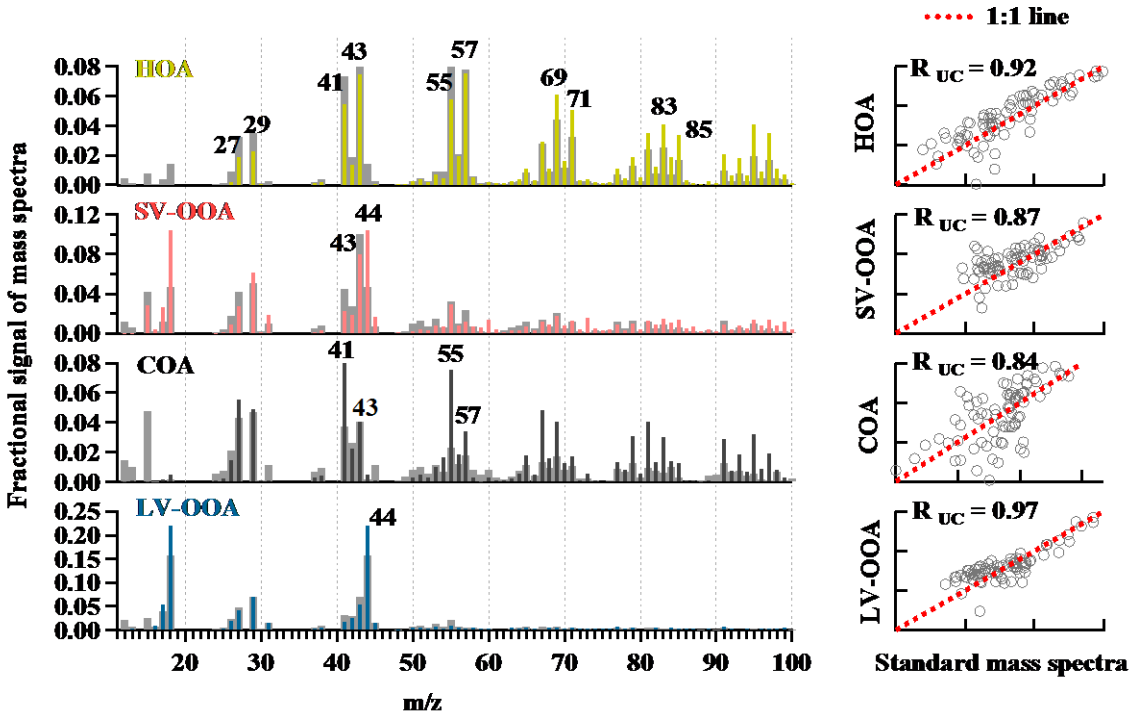

620

621 **Figure 3.** Mass spectra of resolved OA components (HOA, SV-OOA, LV-OOA, COA) with the corresponding standard spectra
622 (in gray) and the correlation with standard mass spectral profiles available on the AMS MS database (Ulbrich, I. M., Lechner,
623 M., and Jimenez, J. L., AMS Spectral Database). The x and y axes in the right-hand graphs are mass spectra of resolved factor
624 and the standard, respectively.

625

626 9) It is not clear that Figure 7 adds that much to the discussion. The conclusions from these figures could
627 be stated in words in a few sentences

628

629 Figure 7 serves as an illustration of the comprehensive effect of Ox and temperature on the concentrations
630 of the OA components. We agree that these conclusions from Figure 7 could be stated in words, but
631 consider a Figure easier to interpret.

632

633 10) Figure captions for Figure 9 and Figure 10. Please clarify what you mean when you say that the data
634 is binned with a range of 7 ug/m3. This is not clear

635 We will modify the caption of Figure 9 and Figure 10 as detailed below.

Page 19443, caption, *addition to main manuscript*:

All the mass concentrations and fractions of above species were sorted according to the hourly average NR-PM1 mass in ascending order. The solid circles represent the average value for each concentration bin with a width of 7 μg m^{-3} , and the vertical lines represent the standard deviations.

Page 19444, caption, *addition to main manuscript*:

All the mass concentrations and fractions of above species were sorted according to the daily average NR-PM1 mass in ascending order. The solid circles represent the average values for each concentration bin with a width of 7 μg m^{-3}, and the vertical lines represent the standard deviations.

Continuous measurements at the urban roadside in an Asian Megacity by Aerosol Chemical Speciation Monitor (ACSM): Particulate matter characteristics during fall and winter seasons in Hong Kong

Chengzhu Sun[1], Berto P. Lee[1], Dandan Huang[2],Yong Jie Li[1,+], Misha I. Schurman[1], Peter K. K. Louie[3], Connie Luk[3] and Chak K. Chan[1,2*]

[1] Division of Environment, Hong Kong University of Science and Technology, Kowloon, Hong Kong, China

[2] Department of Chemical and Biomolecular Engineering, Hong Kong University of Science and Technology, Kowloon, Hong Kong, China

[3] Hong Kong Environmental Protection Department, Wan Chai, Hong Kong, China

*Corresponding author: Chak K. Chan (keckchan@ust.hk) keckchan@ust.hk

[+] Current Address: School Faculty of Engineering and Applied Science, Harvard and Technology, University, Cambridge, MA 02138, USA of Macau, Macau, China

Abstract

Non-refractory submicron aerosol is characterized using an Aerosol Chemical Speciation Monitor (ACSM) in the fall and winter seasons of 2013 at the roadside in an Asian megacity environment in Hong Kong. Organic aerosol (OA), characterized by application of Positive Matrix Factorization (PMF), and sulfate are found dominant. Traffic-related organic aerosol shows good correlation with other vehicle-related species, and cooking aerosol displays clear meal-time concentration maxima and association with surface winds from restaurant areas. Contributions of individual species and OA factors to high NR-PM_1 are analyzed for hourly data and daily data; while cooking emissions in OA contribute to high hourly concentrations, particularly during meal times, secondary organic aerosol components are responsible for episodic events and high day-to-day PM concentrations. Clean periods are either associated with precipitation, which reduces secondary OA with a lesser impact on primary organics, or clean oceanic air masses with reduced long-range transport and better dilution of local pollution. Haze events are connected with increases in contribution of secondary organic aerosol, from 30% to 50% among total non-refractory organics, and influence of continental air masses.

1 Introduction

The Special Administrative Region of Hong Kong (HKSAR) is a global logistics and finance center located at the south-eastern edge of the Pearl River Delta Region (PRD), China's largest manufacturing area and one of the world's most densely populated regions. Hong Kong has been plagued by deteriorating air quality, attributed to local emissions from traffic, residential and commercial activity, regional pollution from the PRD and long-range transport [(Nie et al., 2013; Wong et al., 2013; Yuan et al., 2013).]

High-time-resolution, online instruments can characterize ambient aerosols quickly and mitigate the influence of changing environmental conditions. Few real-time studies have been conducted in Hong Kong aside from recent measurement campaigns conducted by high resolution aerosol mass spectrometer (HR-AMS) [(Lee et al., 2013; Li et al., 2013; Li et al., 2015; Huang et al., 2015).] Long-term AMS studies tend to be costly and time-consuming due to the complexity of the instrument. The ACSM, whose design is based on the AMS but has been substantially simplified, has seen a growing trend of use due to its comparative ease of operation, robustness, and sufficient time resolution (~20-60min) for studies spanning months or longer. ((Ng et al., 2011; Sun et al., 2012, 2013a, b; Budisulistiorini et al., 2013; Canonaco et al., 2013; Takahama et al., 2013; Bougiatioti et al., 2014; Petit et al., 2014)2015; Ripoll et al., 2014a)2015; Tiitta et al., 2014; Minguillón et al., 2015).]

~~This study presents the first ACSM characterization of particulate matter at a busy urban roadside station in Hong Kong with heavy traffic and commercial and residential activities. It aims to provide long-term characterization of particulate matter sources in a typical inner-city environment, enabling the identification of the relative importance of different sources and typical recurring patterns.~~

A high resolution aerosol mass spectrometer (HR-ToF-AMS) had been previously deployed at an urban site in the Shenzhen metropolitan area and a rural site in the PRD region in the fall months of October and November (He et al., 2011; Huang et al., 2011). They found that organic constituents dominate, followed by sulfate which is similar to this study, but the fraction of sulfate at the rural site is larger than that of the urban site. Four OA components were identified at the urban site including HOA, BBOA, LV-OOA and SV-OOA, but only three OA factors without HOA were resolved at the rural site. They both reported an important contribution from BBOA with about 24% of total OA.

We also have previously deployed an HR-ToF-AMS at the supersite of the Hong Kong University of Science and Technology (HKUST) to determine typical variations in submicron species concentrations, overall composition, size distributions, PMF-resolved organic factors and degree of oxygenation. The supersite measurements provided valuable insights into characteristics of mainly of secondary components of submicron particulate matter, with dominance of sulfate and oxygenated organic aerosol species observed (Lee et al., 2013; Li et al., 2013, 2015). Subsequent work was conducted at a downtown location (Mong Kok) in Hong Kong, next to the roadside, in spring 2013 to assess important primary aerosol sources in the inner-city to identify contributions of long-range transport to roadside pollution, and to establish characteristic concentration trends at different temporal scales. Cooking aerosol was identified as the dominant component in submicron non-refractory organics, followed by traffic-related emissions (Lee et al., 2015).

Different from previous studies in Hong Kong, this work focuses on the characterization of roadside aerosol during the fall and winter seasons, when the influence of transported air mass is greatest and PM pollution in Hong Kong is generally more severe. Episodic haze events were found to be mainly driven by secondary aerosol rather than primary emissions, while hourly high PM concentrations were often driven by cooking aerosol. Statistical methods were employed to show that the correlation of COA and HOA to SV-OOA varied under different conditions and in different times of the day. While HOA showed a stronger relationship to SV-OOA overall, COA can be an important contributor to SV-OOA during meal times.

2. Experimental

The roadside measurement data were collected from 3 September to 31 December, 2013 in Mong Kok (MK), an urban area with dense buildings and population in the Kowloon peninsula ~~as part of a~~under the Hong Kong Environmental Protection Department (HKEPD) project (ref.: 13-00986). The sampling site was next to the road-side air quality monitoring station (AQMS) of HKEPD at the junction of the heavily trafficked Nathan Road and Lai Chi Kok Road (22°19'2"N, 114°10'06"E). The distribution of businesses in the vicinity varies, with restaurants mainly to the east, commercial buildings to the south and east, small shops for interior decoration, furniture and electrical goods to the west and residential buildings to the

north of the sampling location [(Lee et al., 2015, submitted].). The sampling setup is described in detail in the Supporting Information, Section 1.

Non-refractory PM_1 (NR-PM_1) species (sulfate, nitrate, ammonium, chloride, and organics) were measured in-situ by an Aerodyne Aerosol Chemical Speciation Monitor (ACSM, SN: 140-154). Other data including meteorological data (wind, temperature, relative humidity, solar irradiation), volatile organic compounds (VOCs) measured by an online gas-chromatography system (GC955-611 and GC955-811, Synspec BV), and standard criteria pollutants (NO_x, SO_2 and $PM_{2.5}$) were provided by the HKEPD, with equipment details available from the HKEPD air quality reports [(Environmental Protection Department, 2013].).

The acquired 20-minute-average data were treated according to the general ACSM data analysis protocols established in previous studies [(Ng et al., 2011; Sun et al., 2012],), using the standard WaveMetrics Igor Pro-based Data Analysis Software (Version 6.3.5.5) and incorporating calibrations for relative ionization efficiency (RIE), collection efficiency (CE) and detection limit (DL). Further details on data treatment can be found in the Supporting Information, Section 2.

Factors contributing to organic aerosol were explored using PMF [(Paatero and Tapper, 1994; Zhang et al., 2011]) with the Igor-Pro-based PMF evaluation toolkit (PET) [(UIbrich et al., 2009].). In general, PMF can be used to resolve factors as organic aerosol (OA) into factors such as hydrocarbon-like OA (HOA), cooking OA (COA), semi-volatile oxygenated OA (SV-OOA), low-volatility oxygenated OA (LV-OOA), and others. ME-2 analysis with the SOFI tool as applied in several studies may yield additional insights but has not been applied in this study due to its ongoing development (Canonaco et al., 2013; Minguillón et al., 2015). The optimal factor number was determined by inter-comparing factors' mass spectra and time series, correlations between factors and related tracers, and correlations with standard mass spectra; solutions with 3, 4, and 5 factors at fpeak= 0 and 6 factors at fpeak= -0.2 were explored, after which the optimal fpeak value was determined by repeating the above analysis with varying fpeak values.

The 4-factor solution (HOA, COA, SV-OOA, LV-OOA) is optimal, with Q/Q_{exp}=0.8 and better differentiation between factor time-series (R_{pr} <0.6; Figure S4Fig. S6). The factors also correlate well with associated inorganics and external tracers (NO_3, SO_4, NH_4, NO_x; Zhang et al., 2005, 2011; Ulbrich et al., 2009), e.g. HOA with NO_x, SV-OOA with NO_3, LV-OOA with SO_4 and NH_4 (Table S4). Furthermore, the resolved mass spectra of four factors exhibit good similarity (all un-centered R (R_{uc}) >0.80) with

reference source mass spectra from the AMS MS database ~~[~~(Ulbrich, I. M., Lechner, M., and Jimenez, J. L., AMS Spectral Database, url: http://cires.colorado.edu/jimenez-group/AMSsd; Ulbrich et al., 2009~~].~~). PMF diagnostic details are shown in the Supplementary Information (SI: Section 3) and ~~Figure S5.We note that *m/z* 60 and 73 were resolved not only in COA but also in SV-OOA. When PMF was run using only nighttime data (between 0:00 and 6:00), when there is little COA (Figure S6), these two ions still persist, with similar fractional intensities in SV-OOA as at other times. The time series of *m/z* 60 and 73 also track well with SV-OOA, with R_{pr} of 0.92 and 0.93 respectively; hence, we believe that their presence in SV-OOA is not the result of artifacts in PMF~~Fig. S7.

We note that m/z 60 and 73, important makers of BBOA mass spectra (Aiken et al., 2010; Cubision et al., 2011; Huang et al., 2011), were resolved not only in COA but also in SV-OOA. Their presence in SV-OOA is not the result of artifacts from the PMF analysis, but were attributed to the following reasons, with more details shown in the supplement (Sect.4-6). Firstly, when PMF was run using only nighttime data (between 0:00 and 6:00), i.e. when there is little COA (Fig. S10), these two ions still persist with similar fractional intensities in SV-OOA as at other times. Secondly, increasing the number of PMF factors and adjusting the fpeak value did not yield a distinct satisfactory BBOA factor. Thirdly, the time series of *m/z* 60 and 73 show weak correlation with other burning tracers (EC_residual, CO_residual), with Rpr of about 0.2 and 0.4 respectively, but track well with SV-OOA, with R_{pr} of 0.92 and 0.93 respectively (Fig. S12, Table S9).

In terms of the possible sources of *m/z* 60 and 73, we observe that these two ions showed matching peaks with the COA diurnal profile and good correlations with the sum of the time series of COA and LV-OOA, with R_{pr} of 0.72 and 0.78 respectively. Furthermore, the ratio of the integrated signal at m/z 60 to the total signal in the organic component mass spectrum is 0.48%, which is just slightly higher than the baseline level (0.3%±0.06%) observed in environments without biomass burning influence and with SOA dominance in ambient OA (Cubision et al.,2011). This indicates that these two ions at Mong Kok were mainly imbedded in cooking emissions and background aerosol due to transport rather than in a distinct source with further details shown in the supplement (Sect. 6).

3 Results and discussion

3.1 Mass concentration and chemical composition

~~Figures~~Figure 1a and 1b display meteorological data (relative humidity, temperature, and precipitation) and mass concentrations of non-refractory PM_1 (NR-PM_1) species and organic aerosol (OA) components, respectively, between September and December 2013. Total NR-PM_1 concentrations vary from 2.1 μg/m^3 to 76.4 μg/m^3 with an average of 25.9~~±~~ ± 13.0 μg/m^3. ACSM NR-PM_1 concentrations co-vary with that of $PM_{2.5}$ measured by TEOM (R^2=0.64, slope=0.59; ~~Figure~~Fig. S1); the low slope value may be caused by the different size cuts of ACSM and TEOM and the presence of refractory materials such as elemental carbon (and to a lesser extent mineral dust and sea salt) which the ACSM cannot detect. Overall, daily $PM_{2.5}$ concentrations range from 3.7 μg/m^3 to 106.0 μg/m^3 and are largely (90.0%) within the 24-hr air quality standard of 75 μg/m^3 set by the Hong Kong Air Quality Objectives (HKAQO). Days with better air quality ($PM_{2.5}$<35 μg/m^3) are mainly observed in the month of September and ~~in~~during rainy periods ~~of~~in the other months. The prevailing winds from the ocean in September not only ~~bring~~brings in less polluted air mass but also ~~dilute the~~dilutes local air pollutants more compared with other seasons ~~[~~(Yuan et al., 2006; Li et al., 2015~~].~~). Precipitation has an obvious impact on total NR-PM_1 concentrations, but as we will discuss, has a lesser effect on primary organics.

Overall, NR-PM_1 is dominated by organics and sulfate with relative contributions of 58.2% and 23.3% and average concentrations of 15.1~~±~~ ± 8.1 μg/m^3 and 6.0 ± 3.5 μg/m^3, respectively (~~Figure~~Fig. 2a). Other inorganic species (ammonium, nitrate and chloride) amount to approximately 20% of NR-PM_1. The dominance of organics and sulfate is consistent with previous on-line studies in urban areas ~~[~~(e.g., Salcedo et al., 2006; Aiken et al., 2009; Sun et al., 2012, 2013b~~]~~) as well as previous filter-based studies in MK ~~[~~(e.g., Louie et al., 2005; Cheng et al., 2010 and Huang et al., 2014~~].~~). The measured composition is consistent with earlier HR-AMS measurements carried out at the same site in spring and summer 2013 ~~[~~(Lee et al., 2015~~, submitted]~~) with very similar overall species distribution, but slightly lower measured concentrations as compared to the ACSM~~,~~. This is likely due to the fact that sampling took place in different time periods (spring-summer 2013 for the AMS campaign, fall-winter 2013 for the ACSM campaign). In the AMS study, 6 PMF aerosol factors were identified (one additional OOA factor and one additional COA factor). ~~-~~A marked difference is observed in the distribution of primary OA (POA) and secondary OA (SOA); whereas in spring and summer (AMS), POA makes up 65% of total organics, the reverse is observed for fall and winter (ACSM) where POA only amounts to 42% overall. A possible reason for this discrepancy is the fact that impacts of regional pollution and long-range transport are usually higher during fall and winter ~~[~~(Yuan et al., 2013~~,~~; Li et al., 2015~~],~~), thus contributing more SOA.~~-~~

Elemental carbon (EC) concentrations are significant at the Mong Kok site but not measureable by ACSM due to its high refractory temperature. EC has been discussed extensively in the previously mentioned filter-based studies and a brief comparison of online ECOC measurements to the results of HR-AMS measurements has been presented in ~~an~~the HR-AMS study ~~[~~(Lee et al., 2015~~, submitted].~~). We therefore do not discuss EC in detail in this work.~~——~~

3.2 OA Components

PMF resolved four factors, including two primary OA factors (hydrocarbon-like OA (HOA) from traffic emissions and cooking OA, or COA) and two oxygenated OA factors (OOA): highly oxidized low-volatility OOA (LV-OOA) ~~–~~and the less-oxidized ~~mass spectra are depicted in Figure 3. The mass concentration of primary OA factor semivolatile~~semi-volatile OOA ~~[~~(SV-OOA; Aiken et al., 2008; Jimenez et al., 2009; Tiitta et al., 2014~~]. The s~~). The mass spectra are depicted in Fig. 3. The mass concentrations of primary OA factors (HOA and COA), ~~a surrogate~~surrogates of local emissions, ~~constitutes~~constitute 42% of total organics and ~~is~~are slightly higher than that of LV-OOA (38%; ~~Figure~~Fig. 2b).~~-~~ SV-OOA contributes approximately 20% to total OA and is associated with both the primary organic aerosol sources and LV-OOA (see Sect. 3.2).

3.2.1 Hydrocarbon-like OA (HOA)

~~HOA has an average concentration of 2.7 ±0.98 μg/m^3 (Figure~~ The mass spectrum of HOA is dominated by the $C_nH_{2n-1}^+$ ion series (*m/z* 27, 41, 55, 69, 83, 97), typical of cycloalkanes or unsaturated hydrocarbon, which account for 27% of total peak intensity in the HOA spectrum. The other prominent group is the $C_nH_{2n+1}^+$ ion series (*m/z* 29, 43, 57, 71, 85, 99), typical of alkanes and accounting for 26% of the total peak. This mass spectrum is very similar to the standard HOA spectrum with R_{uc} of 0.92, and its fractions of $C_nH_{2n-1}^+$ and $C_nH_{2n+1}^+$ (27%, 26%) are consistent with standard ones (28%, 27%) (Ng et al., 2011). This HOA spectrum is also consistent with that resolved by HR-ToF-AMS at the HKUST Supersite on the dominance of saturated CxHy-type ions, most notably at *m/z* 43 and 57 (Lee et al., 2013).

HOA has an average concentration of 2.7 ± 0.98 μg/m^3 (Fig. 1b) and shows strong diurnal variations, including a regular decrease to about 1 μg/m^3 during 0:00-5:00 (~~Figure 4f~~Fig. 4h) which is discussed in

3.3 section in detail. In addition, the temporal variation of HOA displays strong correlations with NO_x (R_{pr}=0.69), CO (R_{pr}=0.62) and several VOCs (Pentane, Toluene, Benzene) as shown in Table ~~S6~~S10.

The diurnal patterns of vehicle number, HOA, NO, NO_2, NO_x and traffic-related VOCs (i-pentane, n-pentane, toluene, octane, benzene, i-butane and n-butane) are depicted in ~~Figure~~Fig. 5. Vehicle counting on Lai Chi Kok road next to the sampling site spanned 28 - 31 May 2013 and was provided by HKEPD ~~[~~(Lee et al., 2015~~ submitted].~~). Although these dates are different from our campaign period, they provide a useful reference for the traffic conditions near the site. In general, more gasoline and diesel vehicles are observed during daytime than at night. The decrease of these vehicles during 22:00–4:00 is in agreement with the diurnal profile of HOA (~~Figure~~Fig. 4h). On the other hand, liquefied petroleum gas (LPG) vehicles, which are usually taxis, show slightly higher numbers during 22:00–4:00 at the site. HOA increases sharply from 1.5 μg/m^3 at about 6:00 to the morning peak of 3.6 μg/m^3 at 9:00, and then persists at high concentrations until midnight, including another peak with 3.9 μg/m^3 at 17:00. The diurnal pattern of HOA is consistent with that of NO_x ($NO+NO_2$), which is almost exclusively from vehicle emissions. These results are consistent with the traffic conditions at MK with heavy traffic continuously after 6:00 and rush hours from 7:00 to 11:00 and 16:00 to 19:00. NO_2 is the result of direct emission as well as formation from NO, and it increased during daytime to reach a maximum even higher than that of NO at about 17:00. Concentrations of toluene (a fuel additive) and pentane and octane ~~[~~(significant components in exhaust of petrol vehicles; Huang et al., 2011; Wanna et al., 2008~~]~~) start to increase during the morning rush hour (7:00) and peak between 18:00 and 19:00. HOA and NO_x show a distinct morning peak at ~8:00 when a small shoulder is also found in the VOCs. Butane, a constituent of LPG, displays a diurnal pattern different from that of HOA, with higher concentrations between 22:00 and 4:00; LPG-fueled taxis are a major means of transport during the nighttime and early morning, and fuel leakage during refueling may contribute to the observed pattern. ~~Furthermore~~ Furthermore, fuel leakage during refueling of LPG vehicles may contribute more than diesel-fueled vehicular emissions to butane even though the number of diesel fueled vehicles is slightly higher than LPG ones at that time. At last, the sampling site is near a major junction serving a number of district centers (West Kowloon, Sha Tin, Tsim Sha Tsui) and is therefore frequented by taxis.

3.2.2 Cooking-related OA (COA)

~~Figure~~The most prominent ions of the resolved COA profile at MK were *m/z* 41 (mainly C_2HO^+, $C_3H_5^+$) and *m/z* 55 (mainly $C_3H_3O^+$, $C_4H_7^+$). Ratios of *m/z* 41/43 =1.8 and *m/z* 55/57=2.2, which are distinctly larger than that of HOA at 0.73 and 0.76 respectively (Fig. 4); such ratios have been widely reported for COA in AMS and ACSM studies. For example, Lanz et al. (2010) reported ratios of *m/z* 41/43 and *m/z* 55/57 of 0.5 and 0.4 in HOA, and 1.2 and 1.2 in COA, respectively, while Sun et al. (2013a) reported 0.5 for these two ratios in HOA and 2.3 for those in COA, respectively.

Fig. 6a shows COA concentrations sorted by wind direction in MK. The COA concentration reaches up to 12 μg/m^3, contributing ~60% of total organics, when easterly winds dominate, probably due to the large number of restaurants located on the eastern side of the sampling site (~~Figure~~Fig. 6a). In general, COA contributes significantly to the total mass of organic aerosol with an average fraction of 24% (3.7μg/m^3), in line with the 16-30% COA contributions found in several cities including London, Manchester, Barcelona, Beijing, Fresno, and New York ~~[~~(Allen et al., 2010; Huang et al., 2010; Sun et al., 2013b; Mohr et al., 2012; Ge et al., 2012~~]. Figure 7 compares~~). Fig. 6b and c compare the chemical composition of NR-PM_1 and OA during meal times (lunch, 12:00-~~2~~14:00, and dinner, 19:00-21:00) and non-meal times (0:00-6:00); the non-meal period is defined by the periods of low concentration (<2 μg/m^3) in the COA diurnal pattern. During dinner time, the average concentration of organics increases by about 11 μg/m^3 and its contributions in total NR-PM_1 increase to 70%, while the concentrations of other species do not change much (~~Figure~~Fig. 6b). As shown in ~~Figure~~Fig. 6c, the increase in organic concentrations results from the increase in COA from 1.7 to 7.8 μg/m^3 (~360% increase), and to a lesser extent increases in SV-OOA (from 1.5 to 4.5 μg/m^3, a ~200% increase) and in HOA (from 1.4 to 3.2 μg/m^3, a ~130% increase). As shown in Table 1, the average concentration of organics during dinner time is 5 μg/m^3 higher than that during lunch, and this increase is attributed to the increase of COA and SV-OOA mass but not of HOA. This is consistent with the expectation that the cooking activities at MK are higher during dinner than during lunch, while traffic during dinner is comparable to or smaller than that during lunch (~~Figure~~Fig. 4f and ~~Figure~~Fig. 4h). The increase of SV-OOA during dinner time may be the result of enhanced cooking emissions and possibly less evaporation due to lower ambient temperature; contributions from traffic emissions are not likely to be important since there is little increase of HOA during the meal ~~time~~times.

3.2.3 ~~oxygenated~~Oxygenated OA (OOA)

LV-OOA is characterized by the prominent *m/z* 44 ion (mainly CO_2^+) and minor C_nH_{2n-1} and C_nH_{2n+1} ion series generated by saturated alkanes, alkenes and cycloalkanes. The LV-OOA spectrum correlates well with the standard LV-OOA spectrum (~~Figure~~Fig. 3), with a R_{uc} of 0.97. The LV-OOA time series is associated with that of SO_4^{2-} with a R_{pr} of 0.86 (~~Figure~~Fig. 1), consistent with reports in the literature ~~[~~(DeCarlo et al., 2010; He et al., 2011; Zhang et al., 2014; Tiitta et al., 2014~~].~~). The LV-OOA diurnal pattern varies little, suggesting that it is part of the background aerosol, possibly resulting from long range transport (Li et al., 2013; 2015).

SV-OOA, which is less oxidized than LV-OOA, is marked by the dominant ions of *m/z* 43 and *m/z* 44 mainly contributed by $C_2H_3O^+$ and CO_2^+, The mass spectrum of SV-OOA closely resembles that of 'standard' SV-OOA ~~(Figure~~with a R_{uc} of 0.87 (Fig. 3). Some marker fragments of COA and HOA, for example, m/z 41, 43, 55, and 57, are present in the SV-OOA mass spectrum. SV-OOA concentrations are also weakly associated with those of HOA and their co-emitted precursors (benzene and toluene), with R_{pr} of 0.58, 0.65 and 0.51 respectively. In fact, the correlation between SV-OOA and benzene is better than that of HOA and benzene (0.56). The diurnal pattern of SV-OOA also shows peaks at meal times like COA. Lastly, the fraction of signal at *m/z* 44 (*f44* fraction) of SV-OOA at MK is twice that of the standard measured by Q-AMS ~~[~~(Zhang et al., 2014; Tiitta et al., 2014~~].~~). Together, these results suggest that SV-OOA may be correlated with POA (HOA and COA), possibly due to rapid oxidation of POA ~~to~~and semivolatile gases, which may then form SV-OOA. The variation of the average concentration of SV-OOA as a function of binned LV-OOA concentration in increments and a bin width of 2 μg/m^3 is shown in ~~Figure S7~~Fig. S13. The linear, positive relationship between SV-OOA and LV-OOA suggests that non-local formation and subsequent transport may also contribute to the measured SV-OOA at MK. However, it should be mentioned that ACSM resolved organic spectra have been observed to show higher *f44* in other studies (Crenn et al, 2015, Fröhlich et al., 2015) compared to HR-ToF-AMS measurements due to inherent instrumental uncertainties in the determination of *f44*. This might have caused the elevated *f44* observed in our SV-OOA spectrum.

Figure 7 displays the concentration of different OA factors (coded by color) as a function of binned O_x concentration (ppb) and binned temperature (^oC) with a bin width of 15ppb and 5^oC~~,~~ respectively. In general, the concentration of all OA factors increases as O_x increases across all temperatures. While it is understood that LV-OOA and SV-OOA are correlated with O_x because they all result from similar photochemical activities, the correlation between HOA and O_x is the result of the good correlation (0.78)

between HOA and NO_2, which accounts for 84% of total Ox. NO_2 is partly emitted ~~directly~~ from vehicles and partly formed by secondary oxidation at MK as discussed in ~~sect.~~Sect. 3.2.1. Increase in ambient temperature is associated with decrease in HOA and SV-OOA, likely due to evaporation effects and partitioning, but it has no obvious correlations with LV-OOA and COA.

To further assess the relative importance of other OA factors to the resolved SV-OOA, ordinary least squares (OLS) regressions were conducted. Considering the potential influence of primary OA on the regression results, the whole dataset was separated into three time periods consisting of: meal time (MT; 12:00 -14:00, 19:00-21:00) marked by enhanced COA; background time (BT; 0:00-6:00) marked by low POA; and other time (OT; 6:00-12:00, 14:00-19:00 and 21:00-24:00). The data of each period was further divided into high/low temperature (HTemp, LTemp = T<22.5 ^{o}C,) and high/low O_x (HiO_x, LO_x = O_x < 70ppb) to reveal impacts of temperature and the degree of oxygenation on the correlations among OA factors.

Tables 2 and 3 show the coefficients of HOA, COA and LV-OOA in the regression equation for the reconstructed SV-OOA and their average ~~concentration~~ concentrations during different periods under high/low temperature and high/low O_x~~,~~ respectively. ~~The regression coefficients of HOA and COA during each period under HTemp (Table 2) are much smaller than under LTemp, reflecting a weakening of their relationship with SV-OOA as temperature increases. COA under HTemp during BT does not show relationship with SV-OOA with a coefficient value of 0.~~ The average concentrations of HOA and SV-OOA under HTemp are obviously lower than under LTemp for each period but the concentration of COA ~~varied~~and LV-OOA varies little across different temperatures~~. These results are consistent with those shown in Figure 7. The~~ (Table 2). Considering the stronger correlations between HOA and SV-OOA than between COA and SV-OOA ~~suggest,~~ a stronger and closer temperature dependence of HOA and SV-OOA~~.~~ was revealed. In ~~contrast, the coefficient of LV-OOA does not change much (0.26±0.02) irrespective of temperature ranges and the selected time periods, supporting the idea that LV-OOA is the result of transport instead of local formation.~~ addition, the regression coefficients of HOA and COA during each period under HTemp are much smaller than under LTemp, reflecting a weakening of their relationship with SV-OOA as temperature increases.

~~During BT, COA has~~ Consistent with the ~~lowest concentration (< 2 μg/m^3)~~ discussion of Fig. 7, the concentrations of HOA, SV-OOA and LV-OOA under HiOx are much higher than those under LOx for each period (Table 3). Besides, HOA shows ~~no~~a higher correlation with SV-OOA under ~~LO_x. During MT~~

and OT (6:00-24:00) when traffic emission is high, HOA has larger regression coefficients under HiO_x than under LO_xHiOx due to more intensive oxidation of HOA to SV-OOA. However, LV-OOA shows a reverse trend with smaller coefficients with SV-OOA. It is probable that HiOx conditions favor the conversion of SV-OOA to LV-OOA, leading to smaller coefficient of LV-OOA on SV-OOA. In addition, except for the minor increase in the concentrations of COA, the concentrations of HOA, although overall most LV-OOA and SV-OOA generally increase by more than 50% compared with those under LO_x during each period (Figure 7). is considered to be from transport.

Overall, based on Tables 2 and 3At last, we also can conclude that: 1) the coefficient HOA overall has a stronger relationship to SV-OOA compared to COA, supported by much higher coefficients of HOA is much larger than that of COA over all time periods, and temperature and O_x levels; 2) In the BT periods, the COA concentration is the lowest compared with other periods and had no relationship with SV-OOA under HT or LO_x conditions; 3) COA has the highest average concentration during MT periods but a regression coefficient comparable to those observed in other periods. Thus, HOA overall has a stronger relationship to SV-OOA than COA has.. Cooking emissions reflected by COA are not as important to SV-OOA in the BT periods but they can be important during MT periods. Some SV-OOA might also have converted to LV-OOA under HiO_x, although overall most LV-OOA is considered to be from transport, indicated by the lowest concentration and correlation with SV-OOA during BT, but highest concentration during MT periods.

3.3 Diurnal patterns

The diurnal profiles of NR-PM_1 species and OA components are depicted in FigureFig. 4. Total organics display a diurnal pattern with two pronounced peaks during 12:00-14:00 and 19:00-21:00, corresponding to the peaks of COA at lunch and dinner time respectively. In addition, organics increase at about 10 am, which may be related to the increase of local emissions of HOA and COA by 2.3 μg/m^3 and 1.1 μg/m^3 respectively from 6:00 to 10:00.

The mass concentration of sulfate (FigureFig. 4b) does not show any diel variation. It is likely that sulfate, as a regional pollutant, is mainly formed during long-range transport, leading to the lack of a specific diurnal pattern at MK; a similar flat diurnal pattern for sulfate has also been found at the HKUST supersite in Hong Kong [(Lee et al., 2013; Li et al., 2015].). These results differ significantly from observations in

Beijing and Lanzhou in China and Welgegund in South Africa ~~[~~(Sun et al., 2012, 2013b; Xu et al., 2014; Tiitta et al., 2014~~]~~) where sulfate displays an obvious increase at noon-time in summer and wet seasons due to either photochemical reaction or aqueous oxidation of SO_2. The difference may result from the much lower level of sulfur dioxide (SO_2) with an average of 4.6 ppb in MK compared to for example, ~32 ppb in Beijing, where coal combustion leads to a much higher SO_2 concentration ~~[~~(Lin et al., 2011~~];~~ ~~sulfate~~). Sulfate and relative humidity (RH) have almost no correlation (R^2 =0.06) in MK, suggesting ~~that~~little importance of local aqueous processing ~~may not be significant~~ for the formation of sulfate ~~observed at Mong Kok~~.

Nitrate shows a slight dip around noontime, corresponding to the increase of the ambient temperature (~~Figure~~Fig. 4j~~); evaporative~~). Evaporative loss of particulate nitrate might outweigh the secondary production of nitrate during this time. The diurnal pattern of ammonium (~~Figure~~Fig. 4d) is very similar to that of sulfate, as expected based on their commonly observed association in atmospheric particles. Chloride (~~Figure~~Fig. 4e) has rather low concentrations and shows a similar diurnal variation to that of nitrate, likely due to its volatility.

3.4 Day-of-week patterns

~~Figure~~Fig. 8a shows the average concentration trends on individual days of the week for NR-PM_1 species and ~~Figure~~Fig. 8b describes the diurnal patterns of the OA components for weekdays, Saturdays and Sundays~~, respectively~~. Because of the small datasets on Saturdays and Sundays, data beyond one standard deviation from the mean (25.9~~±~~ ± 13.0 μg/m^3) were removed from the whole dataset to remove the influence of episodic events in this analysis. Overall, total NR-PM_1 concentrations have no obvious variation (average variation less than 5%) from Monday to Saturday, but drop by 16% on Sundays compared to Saturdays. This weekend difference is opposite to the result found in Beijing where higher concentrations ~~occur~~occurred on Sundays than Saturdays ~~[~~(Sun et al., 2013b~~]~~.). On the other hand, ~~some~~ others such as Lough et al. ~~[~~(2006~~]~~) and Rattigan et al. ~~[~~(2010~~]~~) reported that both Saturdays and Sundays had obvious traffic emissions reduction due to less human activities on weekends in Los Angeles and New York~~, respectively~~.

Organics and secondary inorganics (SO_4, NH_4 and NO_3) contributed 54% and 46% respectively to the concentration difference between Sundays and Saturdays in MK. The difference in organics is mainly attributed to the variation of HOA, which shows very similar diurnal variations on Saturdays and weekdays, but has an average decrease of 23% after 7 am on Sundays. A 37% reduction of traffic-related carbonaceous aerosol on Sundays compared with weekdays in MK has been reported ~~[~~(Huang et al., 2014~~].~~). In Hong Kong many people work on Saturday, which leads to a traffic pattern similar to normal weekdays. COA shows nearly the same diurnal patterns on all days, and LV-OOA and SV-OOA do not show obvious variations. Overall, local emissions from traffic contribute most to the day-of-week variations in organics.

3.5 Contributions of individual species and OA factors to high NR-PM_1

~~Figure~~Fig. 9a, 9b ~~and9c~~and 9c show the variation in hourly mass concentration of NR-PM_1 species and OA components and their mass fractions as a function of hourly total NR-PM_1 mass loading~~, respectively.~~. Below 50 µg/m^3, all aerosol species display a nearly linear increase with PM_1 mass loading, with slopes of about 0.5 for organics, 0.25 for sulfate and LV-OOA, and around 0.1 for nitrate, ammonium, COA, HOA and SV-OOA (~~Figure~~Fig. 9a). While the fractions of NH_4 and organics remain relatively stable, sulfate exhibits a decrease and then an increase, and NO_3 and chloride shows a gradual increase then a decrease respectively as NR-PM_1 ~~increased~~increases to 50 µg/m^3 (~~Figure~~Fig. 9b, 9c). Although the mass concentrations of all organic factors increase as NR-PM_1 increases, SV-OOA is the only factor that ~~increased~~increases in mass fraction. Primary OA components (HOA and COA) and transported OA (LV-OOA) show a decrease in fraction and stable contributions respectively as NR-PM_1 increases to 50 µg/m^3, while the contribution of SV-OOA increases sharply from around 5% to 25% of total organic mass. ~~It suggests that SV-OOA plays an important role as NR-PM_1 increases to 50 µg/m^3 in MK. However, beyond~~Beyond 50 µg/m^3, the mass loadings of SO_4 and organics increase, while those of NH_4, NO_3 and LV-OOA remain almost constant, which differs from the observations in Beijing, where NH_4 and NO_3 kept a linear increase from 50 to about 200 µg/m^3 ~~[~~(Sun et al., 2013b; Zhang et al., 2014~~].~~). In terms of fractions, only COA and to a lesser extent SV-OOA, increase as NR-PM_1 increases further. In fact, over 80% of the high hourly NR-PM_1 concentrations (>50 µg/m^3) are observed during the meal-time periods with enhanced cooking activities.

When the hourly averages in ~~Figure~~Fig. 9 are replaced by daily averages (~~Figure~~Fig. 10), the COA concentration varies little and its fraction does not exhibit an increase but instead decreases significantly with increasing daily NR-PM_1. On the other hand, the fractions of SV-OOA and LV-OOA clearly increase. This analysis suggests that while cooking OA is responsible for the hourly high concentrations during meal ~~time~~times and potential high hourly PM levels, LV-OOA/SV-OOA are responsible for episodic events and high day-to-day PM levels.

To analyze the difference in particle composition and meteorological conditions among episodic periods and clean periods, three heavy polluted episodes (19-22, 23-26 Oct and 10-13 Dec) and two clean periods (17-18 Sep and 14-18 Dec), highlighted in ~~Figure 19~~Fig. 1, were analyzed. The average concentrations of these chosen periods are larger than one standard deviation from the average concentration of the campaign (25.9 ±13.0 μg/m^3). The composition, meteorological features (T and RH) and oxidation index (O_x and *f44*) of these five events are shown in Table 4. Clean period 1 (C1) is characterized by low NR-PM_1 concentrations (below 13 μg/m^3), prevailing coastal wind (easterly wind), lack of rain, high ambient temperature (~28 ºC) and high relative humidity (~70%). Another clean period (C2) features continuous precipitation with the coldest and most humid weather condition in the period studied. Haze period 1 (H1) has similar temperature and humidity as C1 but is marked by mixed continental/oceanic winds. From H1 to the following haze period (H2), the observed wind direction shifts to reflect continental transport, with a significant decrease in RH to 36%. Haze period 3 (H3), just before C2, is also dominated by continental winds but with lower temperatures (~19 ºC) than during other haze events.

~~The~~Although the total NR-PM_1 of C1 (12.2 μg/m^3) ~~is~~and C2 (11.8 μg/m^3) are both only 25~~–~~–30% of that during haze periods~~ and this~~, they were driven by different mechanisms. The main differences in meteorological conditions between C1 and C2 are the dominance of continental wind rather than coastal wind, much lower temperature and the existence of precipitation in C2. The low concentration of C1 is mainly attributed to easterly wind bringing less air pollutants and diluting local air pollutants. ~~HOA, COA and SV-OOA in C1 are lower than in C2 despite the lack of rain during C1; their low concentrations during C1 may be~~ To a lesser extent, it is influenced by both particle evaporation ~~during high temperatures, ,~~ especially for SV-OOA, and dilution of local emissions

~~Compared to the adjacent period H3,~~during high temperatures, which might be the reason why HOA, COA and SV-OOA in C1 are lower than in C2 despite the lack of rain. The low mass loading of C2 was mainly caused by the wet deposition of precipitation ~~in C2~~. It dramatically reduces the concentration of secondary species such as SO4, NH4, NO3, SV-OOA and LV-OOA, but not primary HOA and COA.

~~The~~Compared to the adjacent period H3, the total organic mass reduces by 68% to an average of 8.1 μg/m^3 (Table 4). Precipitation effectively removes secondary particles but is less efficient for primary particles that are continuously generated locally.

~~The land-sea breeze observed during H1 (Figure S8) can redistribute PM pollution over the whole PRD~~ With a similar continental source region ~~and accumulate air pollutants effectively [Lo et al., 2006; Chan and Yao, 2008; Lee et al., 2013]. The pronounced high concentration of LV-OOA and SV-OOA, jointly contributing 70% of total organics, reflects the oxidation of primary emissions in the PRD under such cycles, which is also observed at the suburban HKUST site [*Lee et al.*, 2013]. The periodic nitrate peaks in H1 with low concentration in daytime and high concentration in nighttime coincide with temperature changes. In the adjacent H2 period, the prevailing wind is northwesterly and there is a sharp decrease in relative humidity. It is interesting to note that the dip in RH during H2 coincides with the dip in sulfate, ammonium, nitrate and LV-OOA; this might be caused by decreased aqueous-phase processing, and by decreased gas-particle partitioning associated with water uptake under low RH for secondary aerosol particles [*Sun et al.*, 2013a, 2013b].~~

~~The~~ as C2, the most severe pollution event H3 occurred during ~~the H3 period (~~10 ~~–~~ 13 December~~)~~ with an average NR-PM$_1$ of 47.7 μg/~~–~~m^3. ~~This episode is dominated by~~ The persistent northerly wind ~~bringing~~continually brought air masses from the PRD region into Hong Kong and ~~leading~~led to a marked mass increase of secondary species of SO4, NH4, NO3, LV-OOA and ~~SV-OOA~~SVOOA. Furthermore, H3 is characterized by the highest mass concentration and relative contribution of nitrate and SV-OOA compared with other haze periods. This is likely due to the average temperature of H3 being 5~~-6 °C~~ ~~–~~ 6°C lower than that of other haze events.

In addition, although all three haze events have very similar SO4 mass loading, there is a ~ 50% increase in NH4 concentration during the H3 episode, consistent with the increase of nitrate in that period.

The other two haze events are adjacent with influence from both continental and oceanic region in H1 and continental source region in H2. The mixed pattern of source regions during H1 identified as land–sea breeze (Fig. S14) can redistribute PM pollution over the whole PRD region and accumulate air pollutants effectively (Lo et al., 2006; Chan and Yao, 2008; Lee et al., 2013). The pronounced high concentration of LV-OOA and SV-OOA, jointly contributing 70% of total organics, reflects the oxidation of primary emissions in the PRD under such cycles, which is also observed at the suburban HKUST site (Lee et al.,

2013). The periodic nitrate peaks in H1 with low concentration in daytime and high concentration in nighttime coincide with temperature changes. During H2 period, the prevailing wind is northwesterly and there is a sharp decrease in relative humidity. It is interesting to note that the dip in RH during H2 coincides with the dip in sulfate, ammonium, nitrate and LV-OOA; this might be caused by decreased aqueous-phase processing, and by decreased gas-particle partitioning associated with water uptake under low RH for secondary aerosol particles (Sun et al., 2013a, b).

The fractions of ~~m/z 44 among total organics (~~*f*44~~)~~ during these three haze occasions are all lower than that at HKUST ~~[~~(Li et al., 2013~~],~~), which reflects a larger abundance of the less oxygenated POA at the urban MK site. In addition, the POA concentration (HOA+ COA) does not change much between clean periods and haze periods. However, its relative contribution decreases from about 50% during clean periods to 30% during haze events because of the pronounced variation of secondary OA as shown in ~~Figure~~Fig. 11.

4. Conclusions

The characteristics and sources of ambient submicron non-refractory particulate matter (NR-PM_1) were investigated in an urban roadside environment in Hong Kong using an Aerodyne ACSM from September to December, 2013; these are the first ACSM measurements in Hong Kong. Organics and sulfate dominate total NR-PM_1, making up more than 50% and 20% of measured mass concentration, respectively. PMF analysis of organic aerosol mass spectra yielded four characteristic organic aerosol (OA) factors: hydrocarbon-like organic aerosol (HOA), cooking organic aerosol (COA), semi-volatile oxygenated organic aerosol (SV-OOA) and low-volatility oxygenated organic aerosol (LV-OOA). Primary OA factors (HOA and COA) from ~~freshly emission~~fresh emissions contribute 43% of total organics, slightly larger than that of LV-OOA, which is generally a transported pollutant in this study, with about 37% of total organics. SV-OOA contributes about 20% of total organics and is variably correlated with HOA, COA and LV-OOA under different conditions and ~~period~~in different times of ~~a~~ day. While HOA showed a stronger relationship ~~to~~with SV-OOA overall, COA can be an important contributor to SV-OOA during meal times. In addition, the transported pollutants reflected by LV-OOA displays a relatively stable correlation with SV-OOA during ~~the~~ different investigated periods (BT, MT, and OT).

The mass loadings of traffic related aerosol (HOA) are consistent with expected traffic count data and correlate well with various vehicle-related VOCs and NO_x. Furthermore, HOA, with an average decrease of 23% ~~after 7 am~~ on Sundays, ~~contributes most to~~was mainly responsible for the lower organic concentrations on Sundays when compared with other days. Cooking aerosol (COA) displays a well-defined diurnal variation with lunch- and dinner-time peaks and contributes on average 40% of total organics during mealtimes; COA is clearly associated with local easterly winds, which coincides with the ~~placement~~location of nearby ~~restaurant~~restaurants.

The contributions of individual species and OA factors to high NR-PM_1 were analyzed based on hourly data and daily data. ~~It suggests that while~~While cooking is responsible for the hourly high concentrations during meal times, LV-OOA/SV-OOA are responsible for episodic events and high daily PM ~~concentration.~~concentrations. Three heavily polluted episodes and two clean periods were recorded during sampling and attributed to different meteorological and circulatory conditions. The analysis of clean periods shows that precipitation has an obvious deposition impact on total NR-PM_1 concentrations, but has a lesser effect on primary organics. Clean ocean wind not only brings in less polluted air mass, but also dilutes the local air pollutants. During this campaign, high-PM events ~~are~~were generally related to continental air mass influence or land-see breeze circulatory conditions, which has less influence on primary emissions but significant effects on secondary particles, with a pronounced increase in the secondary OA contribution during haze events (from 30% to 50%).

~~**Acknowledgements**~~

~~The Aerodyne Aerosol Chemical Speciation Monitor measurements were part of the Hong Kong Environmental Protection Department (HKEPD) project ref.: 13-00986. Other data including meteorological data, volatile organic compounds (VOCs) and standard criteria pollutants (NOx, SO_2 and $PM_{2.5}$) were kindly provided by the Hong Kong Environmental Protection Department (HKEPD). Funding support for Mr. Berto P. Lee by the Research Grants Council (RGC) of Hong Kong under the Hong Kong PhD Fellowship Scheme (HKPFS) is gratefully acknowledged.~~

~~**Disclaimer**~~

~~The opinions expressed in this paper are those of the author and do not necessarily reflect the views or policies of the Government of the Hong Kong Special Administrative Region, nor does any mention of trade names or commercial products constitute an endorsement or recommendation of their use.~~

Tables

Table 1. Average concentrations of NR-PM_1 and OA components during lunch time, dinner time and non-meal times

Species μg/m^3	Lunch	Dinner	Non-meal
Org	18.8	23.7	10.3
SO_4	5.8	6.1	6.3
NH_4	2.6	2.9	3.0
NO_3	1.4	1.8	1.6
Chl	0.1	0.2	0.2
Organic aerosol components			
HOA	3.2	3.2	1.4
COA	6.2	9.6	1.7
LV-OOA	5.8	5.4	5.6
SV-OOA	3.6	5.5	1.5

Table 2. Regression of SV-OOA ~~on~~vs. HOA, COA and LV-OOA and concentrations of OA factors and O_x under high and low temperature (LT and HT) conditions of the three chosen periods (MT, BT and OT).

Period	Meal time (MT)		Background time (BT)		Other time (OT)	
Temperature	**LTemp**	**HTemp**	**LTemp**	**HTemp**	**LTemp**	**HTemp**
Coefficients [a]						
HOA	0.80	0.56	0.70	0.43	0.48	0.23
COA	0.29	0.15	0.22	0.00	0.31	0.11
~~**LVOOA**~~**LV-**	0.25	0.23	0.23	0.24	0.25	0.28
Adjusted R^2	0.90	0.81	0.83	0.57	0.85	0.73
Average Concentration (μg/m^3, ppb)						
HOA	3.71	2.85	1.60	1.18	3.51	2.88
COA	7.34	7.40	1.61	1.54	3.50	3.74
LV-OOA	5.46	5.57	5.91	5.07	5.85	5.99
SV-OOA	6.30	3.89	2.68	1.44	4.1	2.39
Ox (ppb)	83.12	85.23	58.71	53.45	75.06	76.77

[a] The coefficient of HOA, COA and LV-OOA in the regression equation reconstructing SV-OOA under LTemp (T <22.5 °C) and HTemp (T >22.5 °C) during meal ~~time~~times (12:00-14:00, 19:00-21:00), background time (0:00-6:00) and other

~~time~~times. The average temperature of the whole campaign is 22.5 °C. All entries of coefficients are significant at the 1% level (two-tailed), except that of HOA/OT, which is significant at the 5% level.

Table 3. Regression of SV-OOA ~~on~~vs. HOA, COA and LV-OOA and concentrations of OA factors and Temperature under high and low O_x (HiO_x and LO_x) of ~~three~~the four chosen periods (MT, BT and OT).

	Meal time (MT)		Background time (BT)		Other time (OT)	
	LO_x	HiO_x	LO_x	HiO_x	LO_x	HiO_x
Coefficients [a]						
HOA	0.50	1.13	0.62	0.64*	0.08*	0.52
COA	0.13	0.14	0.00	0.15	0.14	0.14
LV-OOA	0.33	0.10*	0.26	0.18	0.34	0.21
Adjusted R^2	0.73	0.86	0.73	0.80	0.67	0.78
Average Concentration (μg/m³, ppb)						
HOA	2.24	3.41	1.20	2.03	2.11	3.55
COA	7.31	7.57	1.59	1.73	2.77	3.71
LV-OOA	3.50	5.92	5.07	7.22	4.06	6.77
SV-OOA	3.22	5.29	1.85	2.79	1.8	3.56
Temp (°C)	23.30	23.80	21.48	20.39	22.01	22.74

[a] The coefficient of HOA, COA and LV-OOA in the regression equation reconstructing SV-OOA under LO_x (O_x<70 ppb) and HT (O_x>70 ppb) during meal ~~time~~times (12:00-14:00, 19:00-21:00), background time (0:00-6:00) and other ~~time~~times. 70 ppb is the average O_x of the whole study. All entries of coefficients are significant at 1% level (two-level), except those indicated with *, which indicates significance at the 5% level.

Table 4. Measured and calculated parameters in four chosen periods (C1, H1, H2, H3 and C2)

	Clean period 1 (C1)[a]		**Haze period 1 (H1)**		**Haze period 2 (H2)**		**Haze period 3 (H3)**		**Clean period 2 (C2)**	
RH (%)	70.8		65.0		36.4		64.8		84.6	
T **(°C)**	27.6		25.0		23.8		18.7		13.2	
O_x (ppb)	69.6		82.0		99.5		70.4		40.9	
***f*44**	0.114		0.118		0.120		0.108		0.057	
Precip(mm)	0		0		0		0		8.9	
Wind	coastal		continental/oceanic		continental		continental		continental	
(μg/m³, %)	**Conc.**	**Perc.**	**Conc.**	**Perc.**	**Conc.**	**Perc.**	**Conc.**	**Perc.**	**Conc.**	**Perc.**
NR-PM_1	12.2		44.1		39.0		47.7		11.6	
Org	6.7	54.4	25.2	57.2	21.1	54.2	25.1	52.6	8.1	69.6

SO_4	3.8	31.2	11.8	26.8	12.1	30.9	11.4	23.8	1.5	12.8
NH_4	1.2	9.9	4.4	10.1	4.4	11.3	6.5	13.6	1.1	9.4
NO_3	0.4	3.5	2.4	5.6	1.3	3.4	4.4	9.2	0.8	7.3
Chl	0.1	1.0	0.2	0.4	0.1	0.2	0.4	0.8	0.1	0.9
HOA	1.2	18.5	3.8	15.1	3.0	14.4	4.2	16.9	2.1	26.2
COA	2.3	34.8	3.7	14.5	3.3	15.5	3.3	13.1	2.6	31.7
LV-OOA	3.0	44.8	11.5	45.4	10.2	48.4	9.9	39.6	1.8	22.0
SV-OOA	0.1	2.0	6.3	25.0	4.5	21.6	7.6	30.4	1.6	20.1

[a] Average of data from clean days (C1 and C2) and hazy days (H1, H2 and H3). ~~C~~C1: 17-18 September; H1: 19-22 October; H2: 23-26 October; H3: 10-13 December; C2: 14-18 December.

T: temperature; RH: relative humidity; O_x: odd oxygen (O_3 + NO_2) in ppbv; *f*44: fraction of m/z 44 in organic mass spectra.

Figures

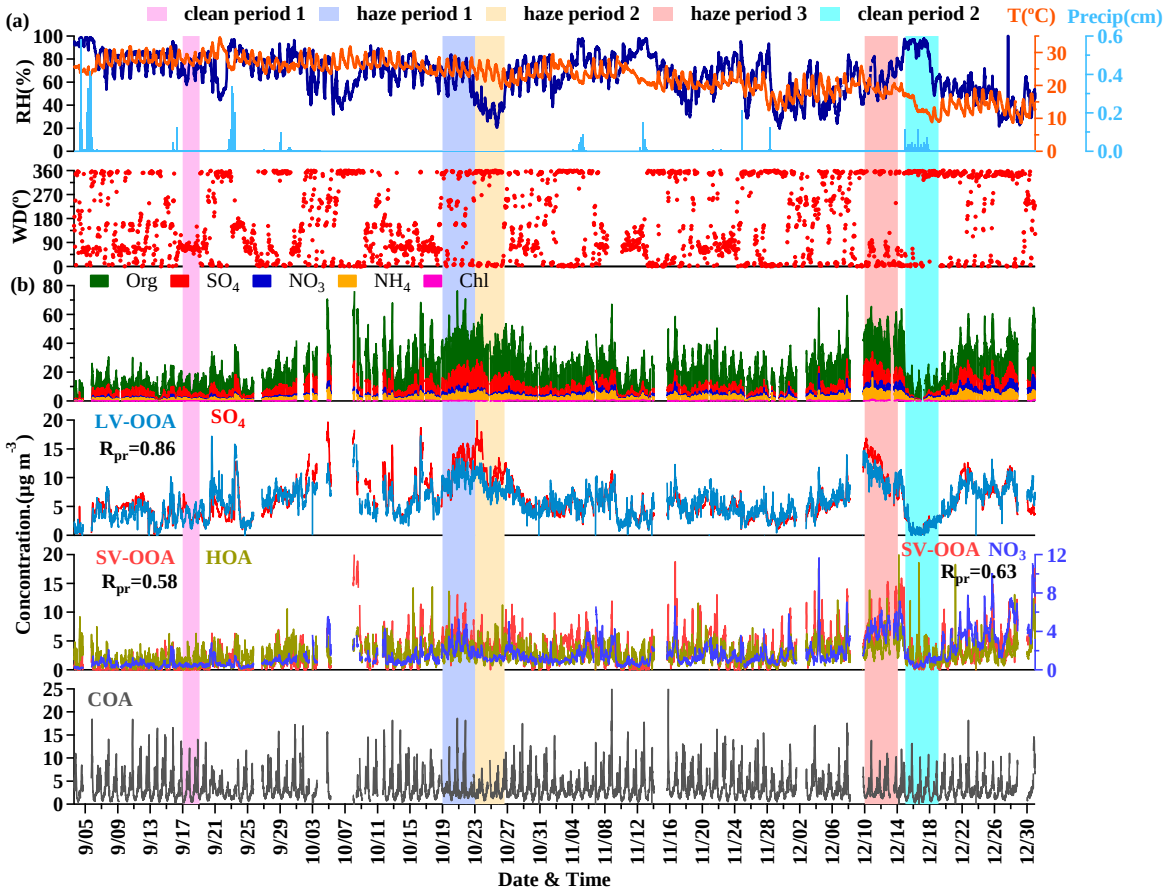

~~Figure~~Fig. **1.** Overview of temporal variation of **(a)** meteorological factors (Relative Humidity, Temperature and Precipitation) and **(b**) stacked plot of non-refractory PM_1 species (Org, SO_4, NO_3, NH_4 and Chl) and non-stacked plot of organic aerosol components (LV-OOA, SV-OOA, HOA and COA). Five periods: clean period 1 (C1), haze period 1 (H1), haze period 2 (H2), haze period 3 (H3) and clean period 2 (C2) are highlighted.

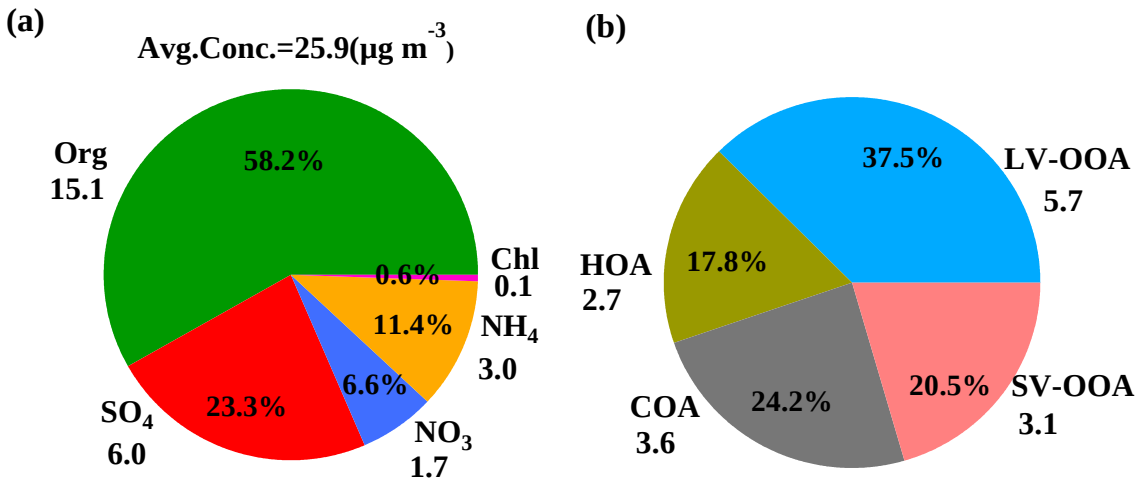

~~Figure~~ Fig. **2**. Average concentration ~~of each~~and chemical composition of **(a)** NR-PM_1 (Org, SO_4, NO_3, NH_4 and Chl) and **(b)** organic aerosol (LV-OOA, SV-OOA, HOA and COA).

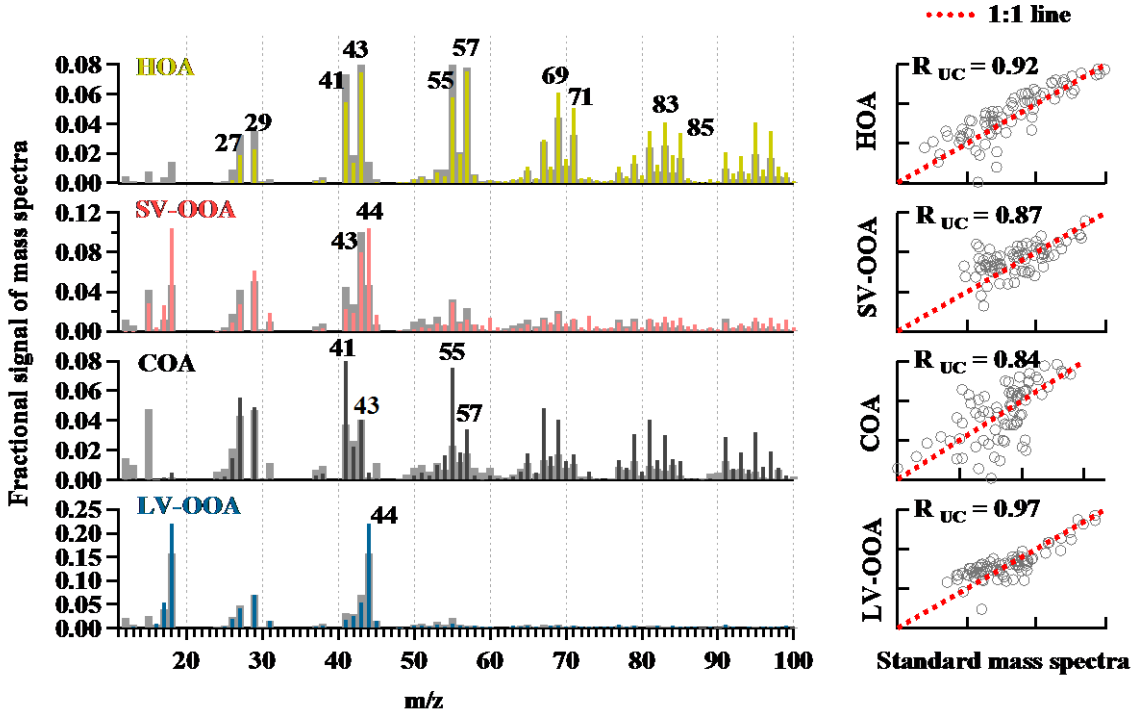

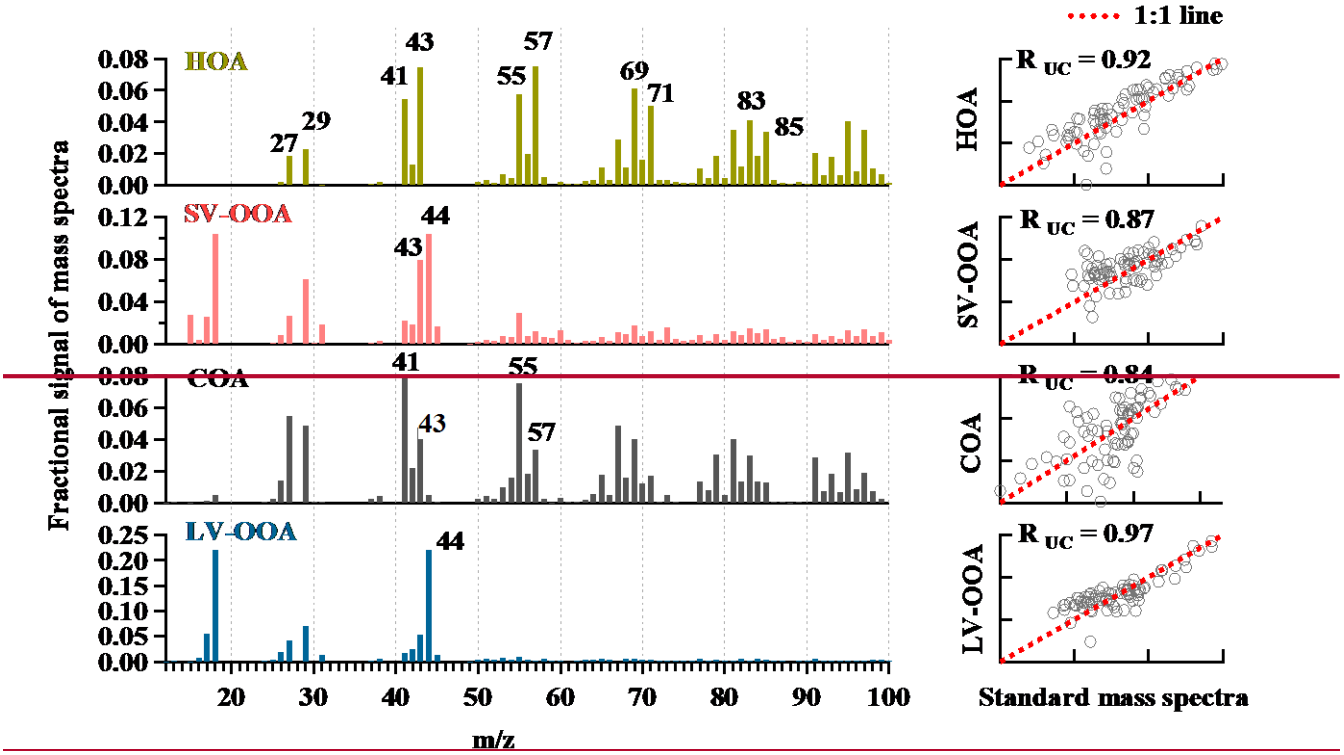

~~Figure~~Fig. 3. Mass spectra of resolved OA components (HOA, SV-OOA, LV-OOA, COA) with the corresponding standard spectra (in gray) and the correlation with standard mass spectral profiles available on the AMS MS database (Ulbrich, I. M., Lechner, M., and Jimenez, J. L., AMS Spectral Database). The x and y axes in the right-hand graphs are mass spectra of resolved factor and the standard, respectively.

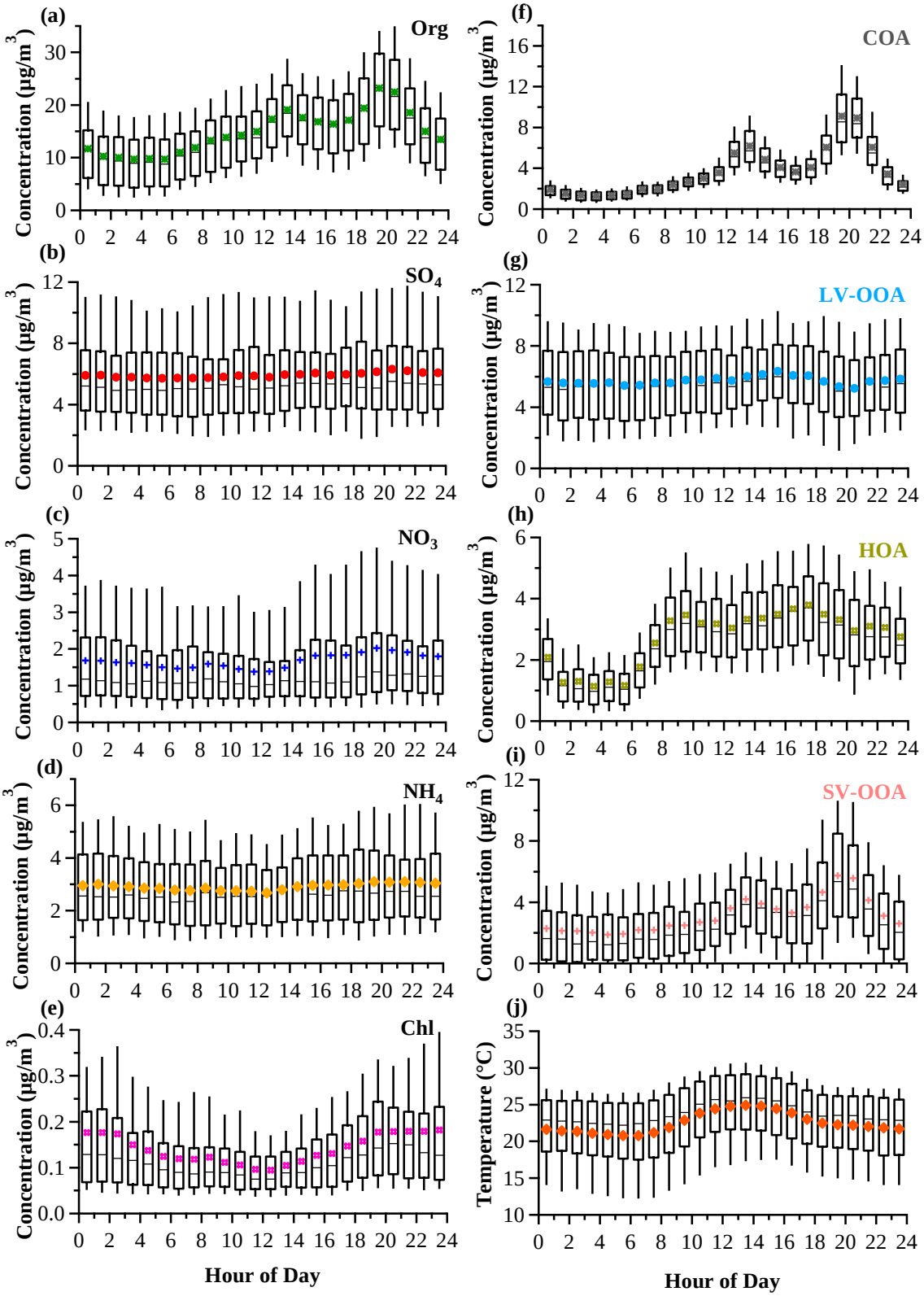

~~Figure~~Fig. 4 Diurnal profiles of NR-PM_1 species, OA components and Temperature for the entire study with 25th and 75th percentile boxes, 10th and 90th percentile whiskers, mean as colored marker and median as black line in the whisker box.

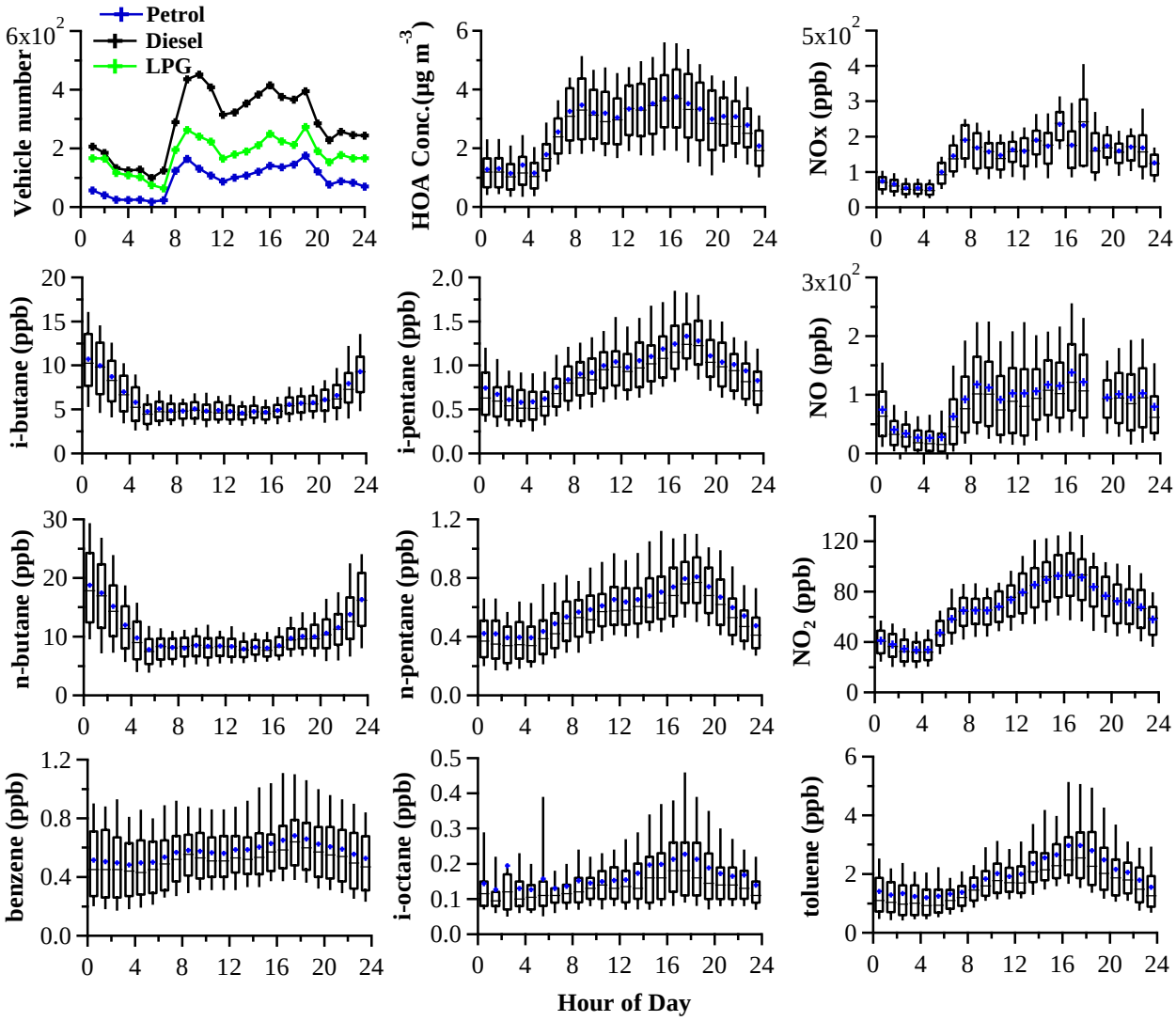

~~Figure~~Fig. 5. Diurnal patterns of vehicle numbers at the Mong Kok site in 28 -31 May 2013 and concentrations of HOA, NO_x, NO_2, NO, i-pentane, n-pentane, i-octane, i-butane, n-butane, benzene and toluene during the whole study.

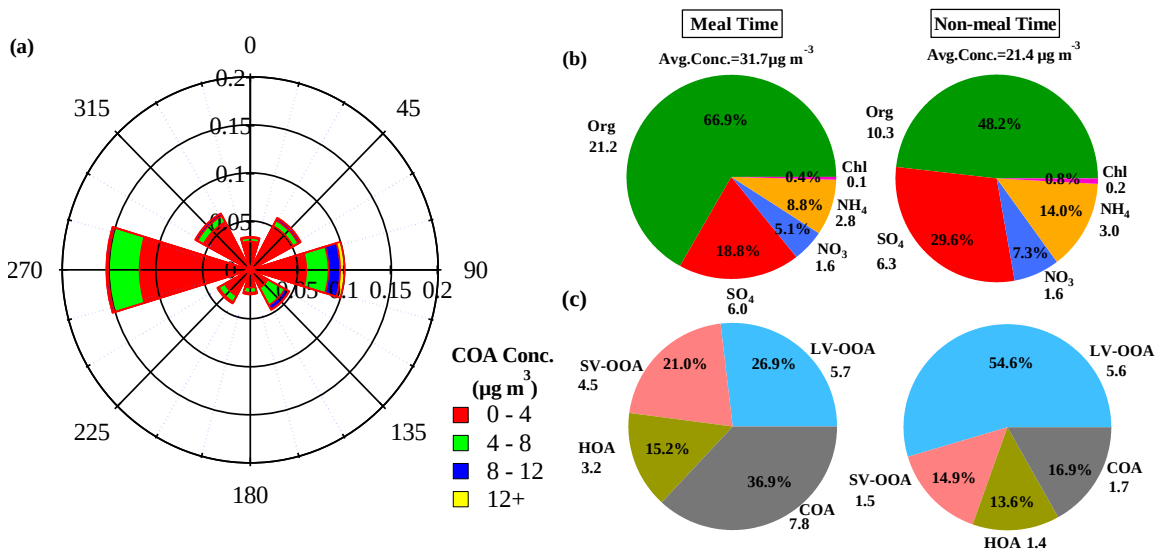

~~Figure~~Fig. 6. (a) Wind rose plot of COA concentration. The angle and radius ~~present~~represent the wind direction and its probability, respectively, while color indicates COA concentration. (b) The fractional composition of NR-PM_1 species during meal ~~time~~times (12:00-2:00, 19:00-21:00) and non-meal time (0:00-6:00). (c) The fractional composition of OA during meal ~~time~~times and non-meal time, respectively.

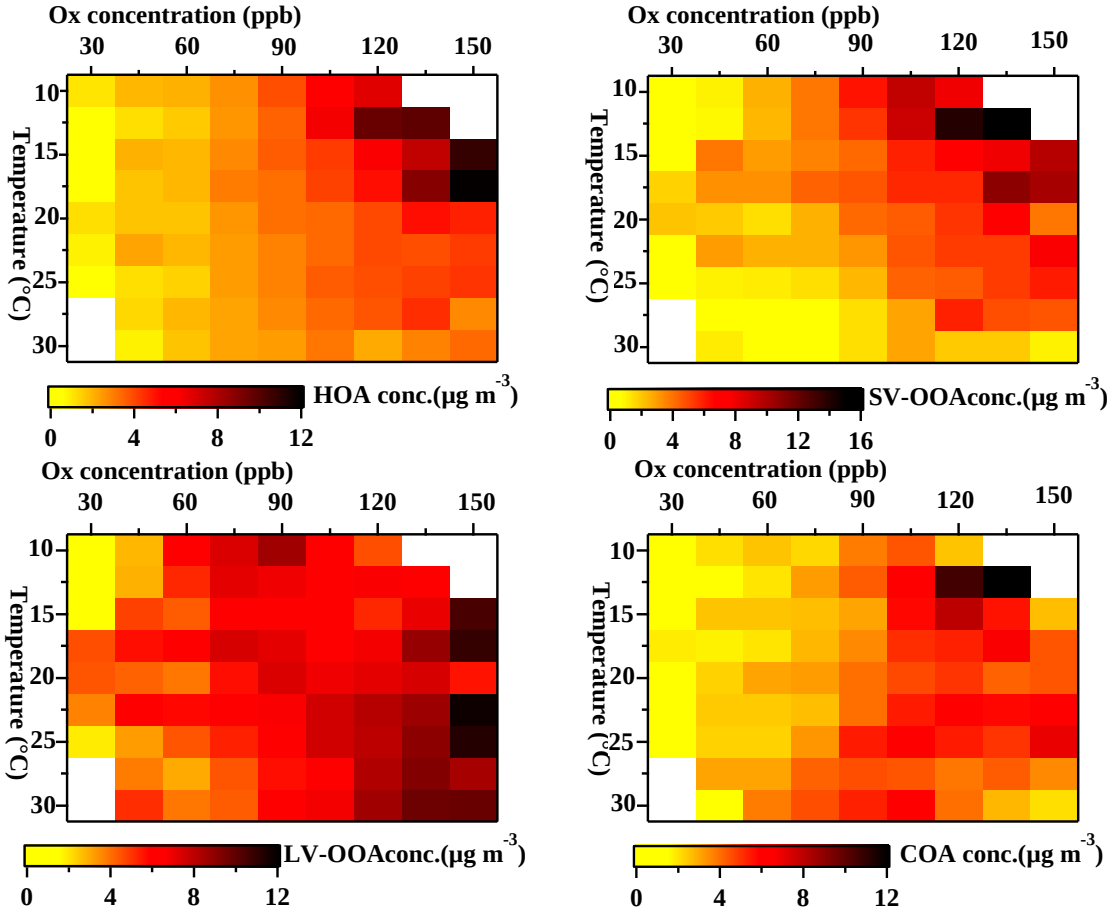

~~Figure~~Fig. 7. Variation of the average concentration of OA components (HOA, SV-OOA, LV-OOA and COA) coded by color as a function of binned O_x concentration (ppb) and binned temperature (°C).

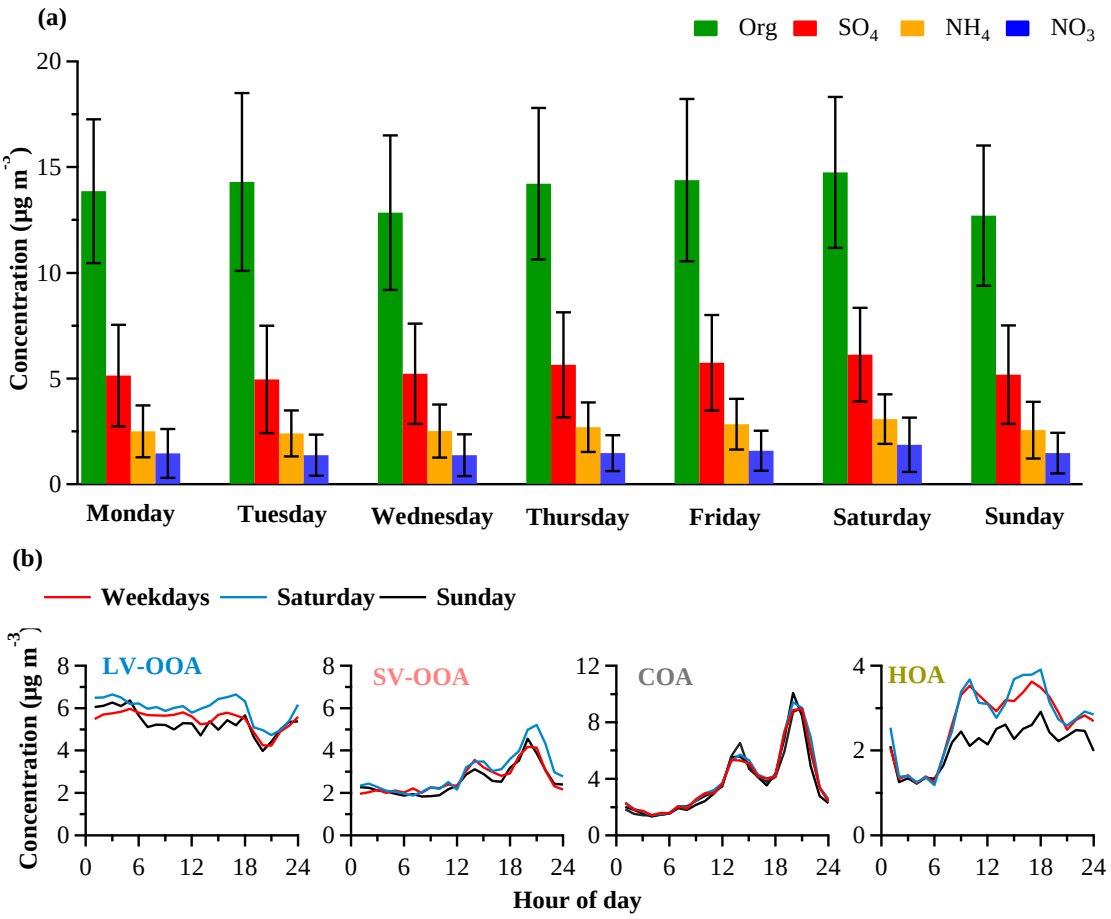

~~Figure~~Fig. 8 **(a)** Day-of-week variations of NR-PM_1 species (standard deviation as vertical line) and **(b)** average diurnal patterns of OA components for weekdays, Saturdays and Sundays.

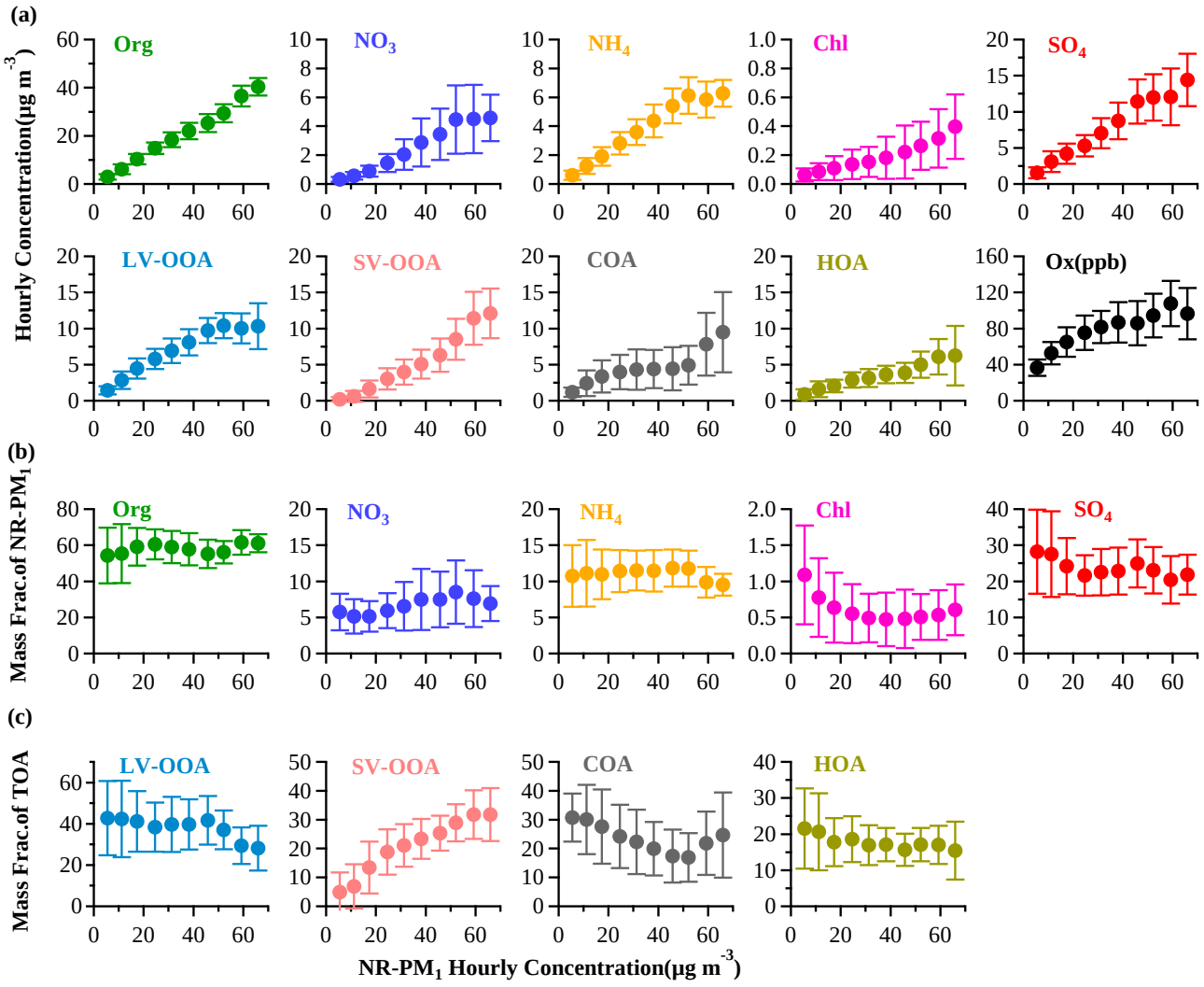

~~Figure~~Fig. **9. (a)** Variation in mass concentration of NR-PM_1 species and OA components as a function of total NR-PM_1 mass loading, and **(b)** mass fraction of total NR-PM_1 for NR-PM_1 species, and **(c)** mass fraction of total organics for OA components, as a function of total NR-PM_1 mass loading. ~~The data~~All the mass concentrations and fractions of above species were ~~binned by~~sorted according to the hourly average NR-PM_1 mass in ascending order. The solid circles represent the average value for each concentration bin with a ~~range~~width of 7 μg/m^3, and the vertical lines ~~are~~represent the standard ~~deviation.~~ deviations.

.

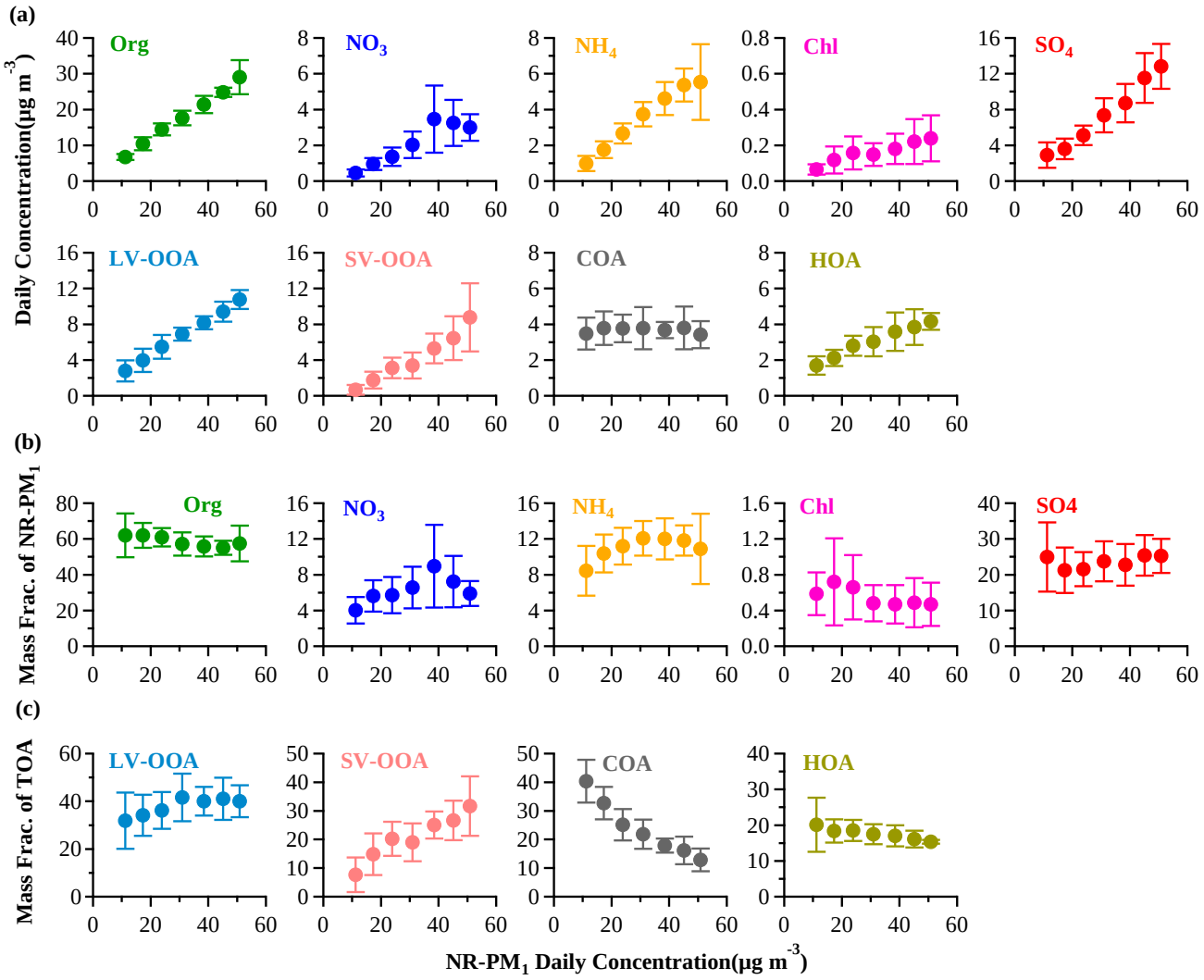

~~Figure~~Fig. **10. (a)** Variation in mass concentration of NR-PM$_1$ species and OA components as a function of total NR-PM$_1$ mass loading, and **(b)** mass fraction of total NR-PM$_1$ for NR-PM$_1$ species, and **(c)** mass fraction of total organics for OA components, as a function of total NR-PM$_1$ mass loading. ~~The data~~All the mass concentrations and fractions of above species were ~~binned by~~sorted according to the daily average NR-PM$_1$ mass in ascending order. The solid circles represent the average

values for each concentration bin with a ~~range~~width of 7 μg/m^3, and the vertical lines ~~are~~represent the standard

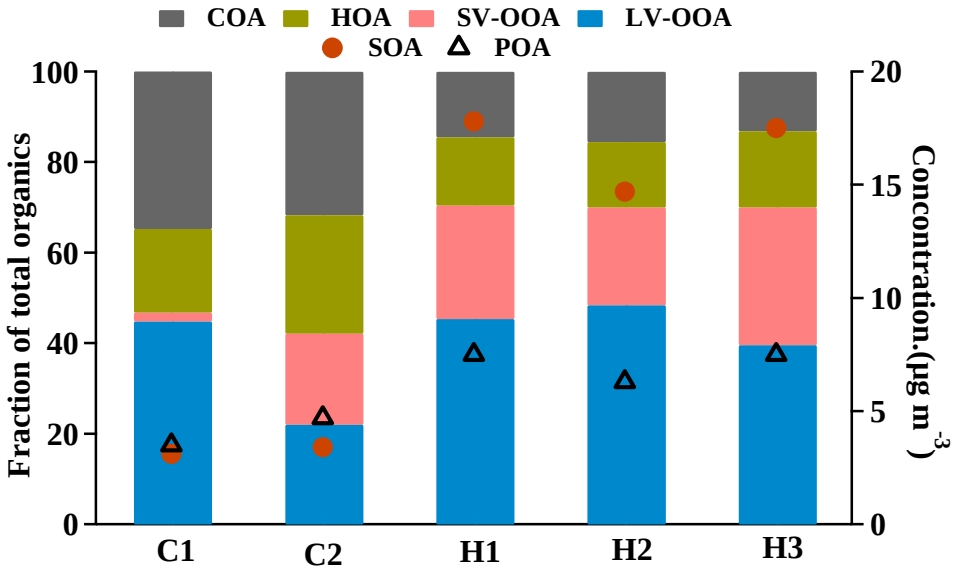

~~deviation.~~deviations.

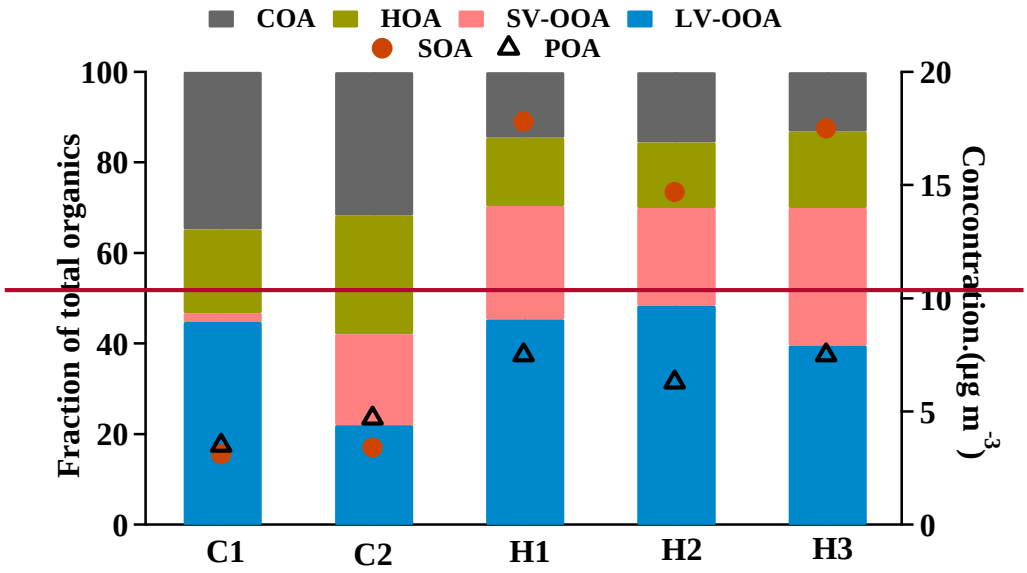

~~Figure11~~**Fig.11.** Mass fraction of hydrocarbon-like organic aerosol (HOA), cooking organic aerosol (COA), semi-volatile oxygenated organic aerosol (SV-OOA) and low-volatility oxygenated organic aerosol (LV-OOA) in color, and the mass concentration of POA and SOA marked by triangles and circles, respectively, during five periods: clean periods (C1 and C2), and haze periods (H1, H2 and H3)

Acknowledgements

The Aerodyne Aerosol Chemical Speciation Monitor measurements were part of the Hong Kong Environmental Protection Department (HKEPD) project ref.: 13-00986. Other data including meteorological data, volatile organic compounds (VOCs) and standard criteria pollutants (NOx, SO_2 and $PM_{2.5}$) were kindly provided by the Hong Kong Environmental Protection Department (HKEPD). Funding support for Berto P. Lee by the Research Grants Council (RGC) of Hong Kong under the Hong Kong PhD Fellowship Scheme (HKPFS) is gratefully acknowledged.

Disclaimer

The opinions expressed in this paper are those of the author and do not necessarily reflect the views or policies of the Government of the Hong Kong Special Administrative Region, nor does any mention of trade

names or commercial products constitute an endorsement or recommendation of their use.

References

Aiken, A. C., DeCarlo, P. F., Kroll, J. H., Worsnop, D. R., Huffman, J. A., Docherty, K. S., Ulbrich, I. M., Mohr, C., Kimmel, J. R., Sueper, D., Sun, Y., Zhang, Q., Trimborn, A., Northway, M., Ziemann, P. J., Canagaratna, M. R., Onasch, T. B., Alfarra, M. R., Prevot, A. S., Dommen, J., Duplissy, J., Metzger, A., Baltensperger, U. and Jimenez, J. L.: O/C and OM/OC Ratios of Primary, Secondary, and Ambient Organic Aerosols with High-Resolution Time-of-Flight Aerosol Mass Spectrometry, Environ. Sci. Technol., 42, 4478-4485, doi: 10.1021/es703009q, 2008.

Aiken, A. C., Salcedo, D., Cubison, M. J., Huffman, J. A., DeCarlo, P. F., Ulbrich, I. M., Docherty, K. S., Sueper, D., Kimmel, J. R., Worsnop, D. R., Trimborn, A., Northway, M., Stone, E. A., Schauer, J. J., Volkamer, R. M., Fortner, E., de Foy, B., Wang, J., Laskin, A., Shutthanandan, V., Zheng, J., Zhang, R., Gaffney, J., Marley, N. A., Paredes-Miranda, G., Arnott, W. P., Molina, L. T., Sosa, G. and Jimenez, J. L.: Mexico City aerosol analysis during MILAGRO using high resolution aerosol mass spectrometry at the urban supersite (T0) – Part 1: Fine particle composition and organic source apportionment, Atmos. Chem. Phys., 9, 6633-6653, doi: 10.5194/acp-9-6633-2009, 2009.

Aiken, A. C., de Foy, B., Wiedinmyer, C., DeCarlo, P. F., Ulbrich, I. M., Wehrli, M. N., Szidat, S., Prevot, A. S. H., Noda, J., Wacker, L., Volkamer, R., Fortner, E., Wang, J., Laskin, A., Shutthanandan, V., Zheng, J., Zhang, R., Paredes-Miranda, G., Arnott, W. P., Molina, L. T., Sosa, G., Querol, X. and Jimenez, J. L.: Mexico city aerosol analysis during MILAGRO using high resolution aerosol mass spectrometry at the urban supersite (T0) – Part 2: Analysis of the biomass burning contribution and the non-fossil carbon fraction. Atmos. Chem. Phys., 10, 5315-5341, doi: 10.5194/acp-10-5315-2010, 2010.

Allan, J. D., Williams, P. I., Morgan, W. T., Martin, C. L., Flynn, M. J., Lee, J., Nemitz, E., Phillips, G. J., Gallagher, M. W. and Coe, H.: Contributions from transport, solid fuel burning and cooking to

primary organic aerosols in two UK cities, Atmos. Chem. Phys., 10, 647-668, doi: 10.5194/acp-10-647-2010, 2010.

Bougiatioti, A., Stavroulas, I., Kostenidou, E., Zarmpas, P., Theodosi, C., Kouvarakis, G., Canonaco, F., Prévôt, A. S. H., Nenes, A., Pandis, S. N. and Mihalopoulos, N.: Processing of biomass-burning aerosol in the eastern Mediterranean during summertime, Atmos. Chem. Phys., 14, 4793-4807, doi: 10.5194/acp-14-4793-2014, 2014.

Budisulistiorini, S. H., Canagaratna, M. R., Croteau, P. L., Marth, W. J., Baumann, K., Edgerton, E. S., Shaw, S. L., Knipping, E. M., Worsnop, D. R., Jayne, J. T., Gold, A. and Surratt, J. D.: Real-Time Continuous Characterization of Secondary Organic Aerosol Derived from Isoprene Epoxydiols in Downtown Atlanta, Georgia, Using the Aerodyne Aerosol Chemical Speciation Monitor, Environ. Sci. Technol., 47, 5686-5694, doi: 10.1021/es400023n, 2013.

Canonaco, F., Crippa, M., Slowik, J. G., Baltensperger, U. and Prévôt, A. S. H.: SoFi, an IGOR-based interface for the efficient use of the generalized multilinear engine (ME-2) for the source apportionment: ME-2 application to aerosol mass spectrometer data, Atmos. Meas. Tech., 6, 3649-3661, doi: 10.5194/amt-6-3649-2013, 2013.

Chan, C. K. and Yao, X. H.: Air pollution in mega cities in China. Atmos. Environ., 42, 1-42, doi: 10.1016/j.atmosenv.2007.09.003, 2008.

Cheng, Y., Ho, K. F., Lee, S. C. and Law, S. W.: Seasonal and diurnal variations of PM1.0, PM2.5 and PM10 in the roadside environment of hong kong, China Particuology, 4, 312-315, doi: 10.1016/s1672-2515(07)60281-4, 2006.

Cheng, Y., Lee, S. C., Ho, K. F., Chow, J. C., Watson, J. G., Louie, P. K. K., Cao, J. J. and Hai, X.: Chemically-speciated on-road PM2.5 motor vehicle emission factors in Hong Kong, Sci. Total Environ., 408, 1621-1627, doi: 10.1016/j.scitotenv.2009.11.061, 2010.

Crenn, V., Sciare, J., Croteau, P. L., Verlhac, S., Fröhlich, R., Belis, C. A., Aas, W., Äijälä, M., Alastuey, A., Artiñano, B., Baisnée, D., Bonnaire, N., Bressi, M., Canagaratna, M., Canonaco, F., Carbone, C., Cavalli, F., Coz, E., Cubison, M. J., Esser-Gietl, J. K., Green, D. C., Gros, V., Heikkinen, L., Herrmann, H., Lunder, C., Minguillón, M. C., Močnik, G., O'Dowd, C. D., Ovadnevaite, J., Petit, J.-E., Petralia, E., Poulain, L., Priestman, M., Riffault, V., Ripoll, A., Sarda-

Estève, R., Slowik, J. G., Setyan, A., Wiedensohler, A., Baltensperger, U., Prévôt, A. S. H., Jayne, J. T., and Favez, O.: ACTRIS ACSM intercomparison – Part I: Reproducibility of concentration and fragment results from 13 individual Quadrupole Aerosol Chemical Speciation Monitors (Q-ACSM) and consistency with Time-of-Flight ACSM (ToF-ACSM), High Resolution ToF Aerosol Mass Spectrometer (HR-ToF-AMS) and other co-located instruments, Atmos. Meas. Tech. Discuss., 8, 7239-7302, doi:10.5194/amtd-8-7239-2015, 2015.

Cubison, M. J., Ortega, A. M., Hayes, P. L., Farmer, D. K., ~~De Gouw, J~~Day, D., Lechner, M. J., Brune, W. H., Apel, E., Diskin, G. S., Fisher, J. A., Fuelberg, H. E., Hecobian, A., Knapp, D. J., Mikoviny, T., Riemer, D., Sachse, G. W., Sessions, W., Weber, R. J., Weinheimer, A. J., Wisthaler, A. and Jimenez, J. L.: Effects of aging on organic aerosol from open biomass burning smoke in aircraft and laboratory studies, Atmospheric Chemistry and Physics, 11, 12049-12064, doi: 10.5194/acp-11-12049-2011, 2011.

~~. and Jimenez, J. L.: Organic Aerosols in the Earth's Atmosphere, Environ. Sci. Technol., 43, 7614-7618, doi: 10.1021/es9006004, 2009.~~

DeCarlo, P. F., Ulbrich, I. M., Crounse, J., de Foy, B., Dunlea, E. J., Aiken, A. C., Knapp, D., Weinheimer, A. J., Campos, T., Wennberg, P. O. and Jimenez, J. L.: Investigation of the sources and processing of organic aerosol over the Central Mexican Plateau from aircraft measurements during MILAGRO, Atmos. Chem. Phys., 10, 5257-5280, doi:10.5194/acp-10-5257-2010, 2010.

Fröhlich, R., Crenn, V., Setyan, A., Belis, C. A., Canonaco, F., Favez, O., Riffault, V., Slowik, J. G., Aas, W., Aijälä, M., Alastuey, A., Artiñano, B., Bonnaire, N., Bozzetti, C., Bressi, M., Carbone, C., Coz, E., Croteau, P. L., Cubison, M. J., Esser-Gietl, J. K., Green, D. C., Gros, V., Heikkinen, L., Herrmann, H., Jayne, J. T., Lunder, C. R., Minguillón, M. C., Močnik, G., O'Dowd, C. D., Ovadnevaite, J., Petralia, E., Poulain, L., Priestman, M., Ripoll, A., Sarda-Estève, R., Wiedensohler, A., Baltensperger, U., Sciare, J., and Prévôt, A. S. H.: ACTRIS ACSM intercomparison – Part 2: Intercomparison of ME-2 organic source apportionment results from 15 individual, co-located aerosol mass spectrometers, Atmos. Meas. Tech., 8, 2555-2576, doi:10.5194/amt-8-2555-2015, 2015.

Ge, X., Setyan, A., Sun, Y. and Zhang, Q.: Primary and secondary organic aerosols in Fresno, California during wintertime: Results from high resolution aerosol mass spectrometry, J. Geophys. Res., 117, D19301, doi: 10.1029/2012jd018026, 2012.

He, L. Y., Huang, X. F., Xue, L., Hu, M., Lin, Y., Zheng, J., Zhang, R. and Zhang, Y. H.: Submicron aerosol analysis and organic source apportionment in an urban atmosphere in Pearl River Delta of China using high-resolution aerosol mass spectrometry, J. Geophys. Res., 116, D12304, doi: 10.1029/2010jd014566, 2011.

Huang, D. D., Li, Y. J., Lee, B. P. and Chan, Ch. K.: Analysis of Organic Sulfur Compounds in Atmospheric Aerosols at the HKUST Supersite in Hong Kong Using HR-ToF-AMS, Environ. Sci. Technol., 49, 3672-3679, doi: 10.1021/es5056269, 2015.

Huang, X. F., He, L. Y., Hu, M., Canagaratna, M. R., Sun, Y., Zhang, Q., Zhu, T., Xue, L., Zeng, L. W., Liu, X. G., Zhang, Y. H., Jayne, J. T., Ng, N. L. and Worsnop, D. R.: Highly time-resolved chemical characterization of atmospheric submicron particles during 2008 Beijing Olympic Games using an Aerodyne High-Resolution Aerosol Mass Spectrometer, Atmos. Chem. Phys., 10, 8933-8945, doi: 10.5194/acp-10-8933-2010, 2010 .

Huang, X. F., He, L. Y., Hu, M., Canagaratna, M. R., Kroll, J. H., Ng, N. L., Zhang, Y. H., Lin, Y., Xue, L., Sun, T. L., Liu, X. G., Shao, M., Jayne, J. T. and Worsnop, D. R.: Characterization of submicron aerosols at a rural site in Pearl River Delta of China using an Aerodyne High-Resolution Aerosol Mass Spectrometer, Atmos. Chem. Phys., 11, 1865-1877, doi: 10.5194/acp-11-1865-2011, 2011.

Huang, X. H. H., Bian, Q. J., Louie, P. K. K. and Yu, J. Z.: Contributions of vehicular carbonaceous aerosols to PM2.5 in a roadside environment in Hong Kong, Atmos. Chem. Phys., 14, 9279-9293, doi: 10.5194/acp-14-9279-2014, 2014.

Huang, Y., Ho, S. S. H., Ho, K. F., Lee, S. C., Yu, J. Z., and Louie, P. K. K.: Characteristics and health impacts of VOCs and carbonyls associated with residential cooking activities in Hong Kong, J. Hazard. Mater., 186, 344-351, http://dx.doi.org/10.1016/j.jhazmat.2010.11.003, 2011.

Jimenez, J. L., Canagaratna, M. R., Donahue, N. M., Prevot, A. S. H., Zhang, Q., Kroll, J. H., DeCarlo, P. F., Allan, J. D., Coe, H., Ng, N. L., Aiken, A. C., Docherty, K. S., Ulbrich, I. M., Grieshop, A. P., Robinson, A. L., Duplissy, J., Smith, J. D., Wilson, K. R., Lanz, V. A., Hueglin, C., Sun, Y. L.,

Tian, J., Laaksonen, A., Raatikainen, T., Rautiainen, J., Vaattovaara, P., Ehn, M., Kulmala, M., Tomlinson, J. M., Collins, D. R., Cubison, M. J., Dunlea, J., Huffman, J. A., Onasch, T. B., Alfarra, M. R., Williams, P. I., Bower, K., Kondo, Y., Schneider, J., Drewnick, F., Borrmann, S., Weimer, S., Demerjian, K., Salcedo, D., Cottrell, L., Griffin, R., Takami, A., Miyoshi, T., Hatakeyama, S., Shimono, A., Sun, J. Y, Zhang, Y. M., Dzepina, K., Kimmel, J. R., Sueper, D., Jayne, J. T., Herndon, S. C., Trimborn, A. M., Williams, L. R., Wood, E. C., Middlebrook, A. M., Kolb, C. E., Baltensperger, U. and Worsnop, D. R.: Evolution of Organic Aerosols in the Atmosphere, Science, 326, 1525-1529, doi: 10.1126/science.1180353, 2009.

~~Laowagul, W., Yoshizumi,~~

Lanz, V. A., Prévôt, A. S. H., Alfarra, M. R., Weimer, S., Mohr, C., DeCarlo, P. F., Gianini, M. F. D., Hueglin, C., Schneider, J., Favez, O., D'Anna, B., George, C. and Baltensperger, U.: Characterization of aerosol chemical composition with aerosol mass spectrometry in Central Europe: an overview, Atmos. Chem. Phys., 10, 10453-10471, doi: 10.5194/acp-10-10453-2010, 2010.

~~K., Mutchimwong, A., Thavipoke, P., Hooper, M., Garivait, H. and Limpaseni, W.: Characterisation of ambient benzene, toluene, ethylbenzene and m-, p- and o-xylene in an urban traffic area in Bangkok, Thailand, International Journal of Environment and Pollution, 36, 241-254, doi: 10.1504/ijep.2009.021829, 2009.~~

Lee, B. P., Li, Y. J., Yu, J. Z., Louie, P. K. K. and Chan, C. K.: Physical and chemical characterization of ambient aerosol by HR-ToF-AMS at a suburban site in Hong Kong during springtime 2011. J. Geophys. Res., 118, 8625-8639, doi: 10.1002/jgrd.50658, 2013.

Lee, B. P., Li, Y. J., Yu, J. Z., Louie, P. K. K. and Chan, C. K.: Characteristics of submicron particulate matter at the urban roadside in downtown Hong Kong – overview of 4 months of continuous high-resolution aerosol mass spectrometer (HR-AMS) measurements, J. Geophys. Res., ~~2015, submitted~~120, 7040-7058, doi: 10.1002/2015JD023311, 2015.

Lee, S. C., Cheng, Y., Ho, K. F., Cao, J. J., Louie, P. K. K., Chow, J. C. and Watson, J. G.: PM 1.0 and PM 2.5 Characteristics in the Roadside Environment of Hong Kong, Environ. Sci. Technol., 40, 157-165, doi: 10.1080/02786820500494544, 2006.

Li, Y. J., Lee, B. Y. L., Yu, J. Z., Ng, N. L. and Chan, C. K.: Evaluating the degree of oxygenation of organic aerosol during foggy and hazy days in Hong Kong using high-resolution time-of-flight aerosol mass spectrometry (HR-ToF-AMS), Atmos. Chem. Phys., 13, 8739-8753, doi: 10.5194/acp-13-8739-2013, 2013.

Li, Y. J., Huang, D. D., Cheung, H. Y., Lee, A. K. Y. and Chan, C. K.: Aqueous-phase photochemical oxidation and direct photolysis of vanillin – a model compound of methoxy phenols from biomass burning, Atmos. Chem. Phys., 14, 2871-2885, doi: 10.5194/acp-14-2871-2014, 2014.

Li, Y. J., Lee, B. P., Su, L., Fung, J. C. H. and Chan, C. K.: Seasonal characteristics of fine particulate matter (PM) based on high-resolution time-of-flight aerosol mass spectrometric (HR-ToF-AMS) measurements at the HKUST Supersite in Hong Kong, Atmos. Chem. Phys., 15, 37-53, doi: 10.5194/acp-15-37-2015, 2015.

Lin, W., Xu, X., Ge, B. and Liu, X.: Gaseous pollutants in Beijing urban area during the heating period 2007–2008: variability, sources, meteorological and chemical impacts, Atmos. Chem. Phys., 11, 8157-8170, doi:10.5194/acp-11-8157-2011, 2011.

Lo, J. C. F., Lau, A. K. H., Fung, J. C. H. and Chen, F.: Investigation of enhanced cross-city transport and trapping of air pollutants by coastal and urban land-sea breeze circulations, J. Geophys. Res., 111, D14104, doi: 10.1029/2005jd006837, 2006.

Lough, G. C., Schauer, J. J. and Lawson, D. R.: Day-of-week trends in carbonaceous aerosol composition in the urban atmosphere. Atmos. Environ., 40, 4137-4149, dio: 10.1016/j.atmosenv.2006.03.009, 2006.

Louie, P. K. K., Chow, J. C., Chen, L. W. Antony, W., John, G., Leung, G. and Sin, D. W. M.: PM2.5 chemical composition in Hong Kong: urban and regional variations, Sci. Total Environ., 338, 267-281, doi: 10.1016/j.scitotenv.2004.07.021, 2005.

Minguillón, M. C., Ripoll, A., Pérez, N., Prévôt, A. S. H., Canonaco, F., Querol, X. and Alastuey, A.: Chemical characterization of submicron regional background aerosols in the Western

Mediterranean using an Aerosol Chemical Speciation Monitor, Atmos. Chem. Phys. Discuss., 15, 965-1000, doi: 10.5194/acpd-15-965-2015, 2015.

Mohr, C., DeCarlo, P. F., Heringa, M. F., Chirico, R., Slowik, J. G., Richter, R., Reche, C., Alastuey, A., Querol, X., Seco, R., Peñuelas, J., Jimenez, J. L., Crippa, M., Zimmermann, R., Baltensperger, U. and Prévôt, A. S. H.: Identification and quantification of organic aerosol from cooking and other sources in Barcelona using aerosol mass spectrometer data, Atmos. Chem. Phys., 12, 1649-1665, doi: 10.5194/acp-12-1649-2012, 2012.

Ng, N. L., Herndon, S. C., Trimborn, A., Canagaratna, M. R., Croteau, P. L., Onasch, T. B., Sueper, D., Worsnop, D. R., Zhang, Q., Sun, Y. L. and Jayne, J. T.: An Aerosol Chemical Speciation Monitor (ACSM) for Routine Monitoring of the Composition and Mass Concentrations of Ambient Aerosol, Aerosol Sci. Tech., 45, 780-794, doi: 10.1080/02786826.2011.560211, 2011.

Nie, W., Wang, T., Wang, W., Wei, X. and Liu, Q.: Atmospheric concentrations of particulate sulfate and nitrate in Hong Kong during 1995–2008: Impact of local emission and super-regional transport. Atmos. Environ., 76, 43-51, doi: 10.1016/j.atmosenv.2012.07.001, 2013.

Paatero, P. and Tapper, U.: Positive matrix factorization: A non-negative factor model with optimal utilization of error estimates of data values, Environmetrics, 5, 111-126, doi: 10.1002/env.3170050203, 1994.

Petit, J. E., Favez, O., Sciare, J., Crenn, V., Sarda-Estève, R., Bonnaire, N., Močnik, G., Dupont, J. C., Haeffelin, M. and Leoz-Garziandia, E.: Two years of near real-time chemical composition of submicron aerosols in the region of Paris using an Aerosol Chemical Speciation Monitor (ACSM) and a multi-wavelength Aethalometer, Atmos. Chem. Phys., 15, 2985-3005, doi: 10.5194/acp-15-2985-2015. 2015.

Rattigan, O. V., Dirk Felton, H., Bae, M. S., Schwab, J. J. and Demerjian, K. L.: Multi-year hourly PM2.5 carbon measurements in New York: Diurnal, day of week and seasonal patterns, Atmos. Environ., 44, 2043-2053, doi: 10.1016/j.atmosenv.2010.01.019, 2010.

Ripoll, A., Minguillón, M. C., Pey, J., Jimenez, J. L., Day, D. A., Sosedova, Y., Canonaco, F., Prévôt, A. S. H., Querol, X. and Alastuey, A.: Long-term real-time chemical characterization of submicron

aerosols at Montsec (southern Pyrenees, 1570 m a.s.l.), Atmos. Chem. Phys., 15, 2935-2951, doi: 10.5194/acp-15-2935-2015, 2015.

Salcedo, D., Onasch, T. B., Dzepina, K., Canagaratna, M. R., Zhang, Q., Huffman, J. A., DeCarlo, P. F., Jayne, J. T., Mortimer, P., Worsnop, D. R., Kolb, C. E., Johnson, K. S., Zuberi, B., Marr, L. C., Volkamer, R., Molina, L. T., Molina, M. J., Cardenas, B., Bernabé, R. M., Márquez, C., Gaffney, J. S., Marley, N. A., Laskin, A., Shutthanandan, V., Xie, Y., Brune, W., Lesher, R., Shirley, T. and Jimenez, J. L.: Characterization of ambient aerosols in Mexico City during the MCMA-2003 campaign with Aerosol Mass Spectrometry: results from the CENICA Supersite, Atmos. Chem. Phys., 6, 925-946, doi: 10.5194/acp-6-925-2006, 2006.

Sun, Y. L., Wang, Z. F., Dong, H. B., Yang, T., Li, J., Pan, X., Chen, P. and Jayne, J. T.: Characterization of summer organic and inorganic aerosols in Beijing, China with an Aerosol Chemical Speciation Monitor, Atmos. Environ., 51, 250-259, doi: 10.1016/j.atmosenv.2012.01.013, 2012.

Sun, Y. L., Wang, Z. F., Fu, P. Q., Jiang, Q., Yang, T., Li, J. and Ge, X.: The impact of relative humidity on aerosol composition and evolution processes during wintertime in Beijing, China, Atmos. Environ., 77, 927-934, doi: 10.1016/j.atmosenv.2013.06.019, 2013a.

Sun, Y. L., Wang, Z. F., Fu, P. Q., Yang, T., Jiang, Q., Dong, H. B., Li, J. and Jia, J. J.: Aerosol composition, sources and processes during wintertime in Beijing, China, Atmos. Chem. Phys., 13, 4577-4592, doi:10.5194/acp-13-4577-2013, 2013b.

Takahama, S., Johnson, A., Guzman Morales, J., Russell, L. M., Duran, R., Rodriguez, G., Zheng, J., Zhang, R., Toom-Sauntry, D. and Leaitch, W. R.: Submicron organic aerosol in Tijuana, Mexico, from local and Southern California sources during the CalMex campaign, Atmos. Environ., 70, 500-512, doi: 10.1016/j.atmosenv.2012.07.057, 2013.

Tiitta, P., Vakkari, V., Croteau, P., Beukes, J. P., van Zyl, P. G., Josipovic, M., Venter, A. D., Jaars, K., Pienaar, J. J., Ng, N. L., Canagaratna, M. R., Jayne, J. T., Kerminen, V. M, Kokkola, H., Kulmala, M., Laaksonen, A., Worsnop, D. R. and Laakso, L.: Chemical composition, main sources and temporal variability of PM1 aerosols in southern African grassland, Atmos. Chem. Phys., 14, 1909—1927, doi: 10.5194/acp-14-1909-2014, 2014.

Ulbrich, I. M., Canagaratna, M. R., Zhang, Q., Worsnop, D. R. and Jimenez, J. L.: Interpretation of organic components from Positive Matrix Factorization of aerosol mass spectrometric data, Atmos. Chem. Phys., 9, 2891-2918, doi: 10.5194/acp-9-2891-2009, 2009.

Wanna, L., Hathairatana, G., Wongpun, L. and Kunio, Y.: Ambient Air Concentrations of Benzene, Toluene, Ethylbenzene and Xylene in Bangkok, Thailand during April-August in 2007, Asian Journal of Atmospheric Environment, 2, 14-25, doi: 10.5572/ajae.2008.2.1.014, 2008.

Wong, T. W., Tam, W. W. S., Yu, I. T. S., Lau, A. K. H., Pang, S. W., and Wong, A. H. S.: Developing a risk-based air quality health index, Atmos. Environ., 76, 52-58, http://dx.doi.org/10.1016/j.atmosenv.2012.06.071, 2013.

Xu, J., Zhang, Q., Chen, M., Ge, X., Ren, J. and Qin, D.: Chemical composition, sources, and processes of urban aerosols during summertime in northwest China: insights from high-resolution aerosol mass spectrometry, Atmos. Chem. Phys., 14, 12593-12611, doi: 10.5194/acp-14-12593-2014, 2014.

Yuan, Z. B., Yu, J. Z., Lau, A. K. H., Louie, P. K. K. and Fung, J. C. H.: Application of positive matrix factorization in estimating aerosol secondary organic carbon in Hong Kong and its relationship with secondary sulfate, Atmos. Chem. Phys., 6, 25-34, doi: 10.5194/acp-6-25-2006, 2006.

Yuan, Z. B., Yadav, V., Turner, J. R., Louie, P. K. K. and Lau, A. K. H.: Long-term trends of ambient particulate matter emission source contributions and the accountability of control strategies in Hong Kong over 1998–2008, Atmos. Environ., 76, 21-31, doi: 10.1016/j.atmosenv.2012.09.026, 2013.

Zhang, Q., Alfarra, M. R., Worsnop, D. R., Allan, J. D., Coe, H., Canagaratna, M. R. and Jimenez, J. L.: Deconvolution and Quantification of Hydrocarbon-like and Oxygenated Organic Aerosols Based on Aerosol Mass Spectrometry, Environ. Sci. Technol., 39, 4938-4952, doi: 10.1021/es048568l, 2005.

Zhang, Q., Jimenez, J. L., Canagaratna, M. R., Ulbrich, I. M., Ng, N. L., Worsnop, D. R. and Sun, Y.: Understanding atmospheric organic aerosols via factor analysis of aerosol mass spectrometry: a review, Analyt. Bioanalyt. Chem., 401, 3045-3067, doi: 10.1007/s00216-011-5355-y, 2011.

Zhang, Y. J., Tang, L. L., Wang, Z., Yu, H. X., Sun, Y. L., Liu, D., Qin, W., Canonaco, F., Prévôt, A. S. H., Zhang, H. L. and Zhou, H. C.: Insights into characteristics, sources, and evolution of submicron aerosols during harvest seasons in the Yangtze River delta region, China, Atmos. Chem. Phys., 15, 1331-1349, doi: 10.5194/acp-15-1331-2015, 2015.

Zhang, Y. M., Zhang, X. Y., Sun, J. Y., Hu, G. Y., Shen, X. J., Wang, Y. Q., Wang, T. T., Wang, D. Z. and Zhao, Y.: Chemical composition and mass size distribution of PM1 at an elevated site in central east China, Atmos. Chem. Phys., 14, 12237-12249, doi: 10.5194/acp-14-12237-2014, 2014.